Check for updates

Received: 23 April 2021 | Revised: 21 June 2021 | Accepted: 25 June 2021

DOI: 10.1002/cne.25204

REVIEW

JCN RESEARCH IN SYSTEMS NEUROSCIENCE THE JOURNAL OF COMPARATIVE NEUROLOGY WILEY

Anatomy and function of retinorecipient arborization fields in zebrafish

Herwig Baier[1] | Mario F. Wullimann[1,2]

[1]Max Planck Institute of Neurobiology, Genes–Circuits–Behavior, Martinsried, Germany

[2]Department Biology II, Division of Neurobiology, Ludwig-Maximilians-University (LMU Munich), Martinsried, Germany

Correspondence
Herwig Baier, Max Planck Institute of Neurobiology, Genes–Circuits–Behavior, Am Klopferspitz 18, 82152 Martinsried, Germany.
Email: hbaier@neuro.mpg.de

Funding information
DFG, Grant/Award Numbers: TP B16, SFB 870; Max Planck Society

Abstract

In 1994, Burrill and Easter described the retinal projections in embryonic and larval zebrafish, introducing the term "arborization fields" (AFs) for the retinorecipient areas. AFs were numbered from 1 to 10 according to their positions along the optic tract. With the exception of AF10 (neuropil of the optic tectum), annotations of AFs remained tentative. Here we offer an update on the likely identities and functions of zebrafish AFs after successfully matching classical neuroanatomy to the digital Max Planck Zebrafish Brain Atlas. In our system, individual AFs are neuropil areas associated with the following nuclei: AF1 with the suprachiasmatic nucleus; AF2 with the posterior parvocellular preoptic nucleus; AF3 and AF4 with the ventrolateral thalamic nucleus; AF4 with the anterior and intermediate thalamic nuclei; AF5 with the dorsal accessory optic nucleus; AF7 with the parvocellular superficial pretectal nucleus; AF8 with the central pretectal nucleus; and AF9d and AF9v with the dorsal and ventral periventricular pretectal nuclei. AF6 is probably part of the accessory optic system. Imaging, ablation, and activation experiments showed contributions of AF5 and potentially AF6 to optokinetic and optomotor reflexes, AF4 to phototaxis, and AF7 to prey detection. AF6, AF8 and AF9v respond to dimming, and AF4 and AF9d to brightening. While few annotations remain tentative, it is apparent that the larval zebrafish visual system is anatomically and functionally continuous with its adult successor and fits the general cyprinid pattern. This study illustrates the synergy created by merging classical neuroanatomy with a cellular-resolution digital brain atlas resource and functional imaging in larval zebrafish.

KEYWORDS
brain atlas, calcium imaging, pretectum, retina, tectum, thalamus, zebrafish

Abbreviations: A, anterior thalamic nucleus; ac, anterior commissure; APN, accessory pretectal nucleus (of Wullimann & Meyer, 1990); ATN, anterior tuberal nucleus; Cer, cerebellum; CP, central posterior thalamic nucleus; CPN, central pretectal nucleus; DAO, dorsal accessory optic nucleus; Di, diencephalon; DiL, diffuse nucleus of the inferior lobe; DiV, diencephalic ventricle; dot, dorsomedial optic tract; DP, dorsal posterior thalamic nucleus; DT, dorsal thalamus (thalamus); E, epiphysis; fr, fasciculus retroflexus; hac, habenular commissure; Had, dorsal habenular nucleus; Hav, ventral habenular nucleus; hc, horizontal commissure; Hd, dorsal zone of periventricular hypothalamus; Hv, ventral zone of periventricular hypothalamus; Hy, hypothalamus; I, intermediate thalamic nucleus; lfb, lateral forebrain bundle; LH, lateral hypothalamic nucleus; LR, lateral recess of diencephalic ventricle; M1, early pretectal migration area; mfb, medial forebrain bundle; MO, medulla oblongata; oc, optic chiasma; ot, optic tract; pc, posterior commissure; PCN, paracommissural nucleus; PGa, anterior preglomerular nucleus; PGl, lateral preglomerular nucleus; PGm, medial preglomerular nucleus; PGZ, periventricular gray zone of optic tectum; PO, posterior pretectal nucleus (of Wullimann & Meyer, 1990); Po, preoptic region; poc, postoptic commissure; PPd, dorsal periventricular pretectal nucleus; PPp, posterior parvocellular preoptic nucleus; PPv, ventral periventricular pretectal nucleus; Pr, pretectum; PSm, magnocellular superficial pretectal nucleus; PSp, parvocellular superficial pretectal nucleus; PTN, posterior tuberal nucleus; PTv, posterior tuberculum, ventral part; PVO, paraventricular organ; SC, suprachiasmatic nucleus; SCO, subcommissural organ; SD, saccus dorsalis; tc, tectal commissure; Tel, telencephalon; TeO, tectum opticum; TeV, tectal ventricle; TLa, torus lateralis; TLo, torus longitudinalis; TN, terminal nerve; tpm, tractus pretectomamillaris; TPp, periventricular posterior tuberular nucleus; VAO, ventral accessory optic nucleus; VL, ventrolateral thalamic nucleus; VM, ventromedial thalamic nucleus; vot, ventrolateral optic tract; VT, ventral thalamus (prethalamus); ZLI, zona limitans intrathalamica.

This is an open access article under the terms of the Creative Commons Attribution License, which permits use, distribution and reproduction in any medium, provided the original work is properly cited.
© 2021 The Authors. *The Journal of Comparative Neurology* published by Wiley Periodicals LLC.

1 | BACKGROUND AND BEGINNINGS

In the first half of the 1990s, there was growing interest in the zebrafish *Danio rerio* (Cyprinidae; formerly *Brachydanio rerio*) as a model animal in the study of the developing teleostean brain. But information on the anatomy of the larval visual system was limited. Burrill and Easter (1994) used the lipophilic carbocyanine dye DiI (1,1′-dioctadecyl-3,3,3′,3′-tetramethylindo-carbocyanine perchlorate) in fixed whole brains—a new tract tracing method at the time (Honig & Hume, 1989)—to report retinal projections in the early zebrafish. This led to the identification of 10 retinal terminal arborization fields (AFs) by observation of fine and beaded arborizations of retinal ganglion cell (RGC) axons in the zebrafish brain (Figure 1). Retinorecipient AFs are defined as neuropil areas that contain spatial clusters of RGC terminals. The AFs gradually emerge between 60 and 72 hours postfertilization (hpf) (Figure 1a–c). Interestingly, during this early period, no pruning of more extensive (transient) retinal projections has been observed. Once established at 3 days postfertilization (dpf), the pattern is stable and does not change qualitatively into late larval and juvenile stages despite substantial tissue growth and addition of newborn RGCs (compare Figure 1c,d). AFs develop into neuropil areas associated with retinorecipient nuclei (RNs). Below we will discuss each of the RNs as described in the classical literature.

Twenty years after Burrill and Easter's landmark study, Robles et al. (2014) generated 3D reconstructions of the retinofugal projections from confocal imaging of transgenic fluorescent reporter lines, largely confirming the original description. Axon tracings were combined with labeling of synaptic terminals with a Synaptophysin-GFP fusion protein driven by an RGC-specific promoter/enhancer (Figure 2). These authors also traced close to 500 individual, stochastically labeled RGC axons to reveal a cellular-resolution "projectome" of the retina. More recently, Kölsch et al. (2021) catalogued the

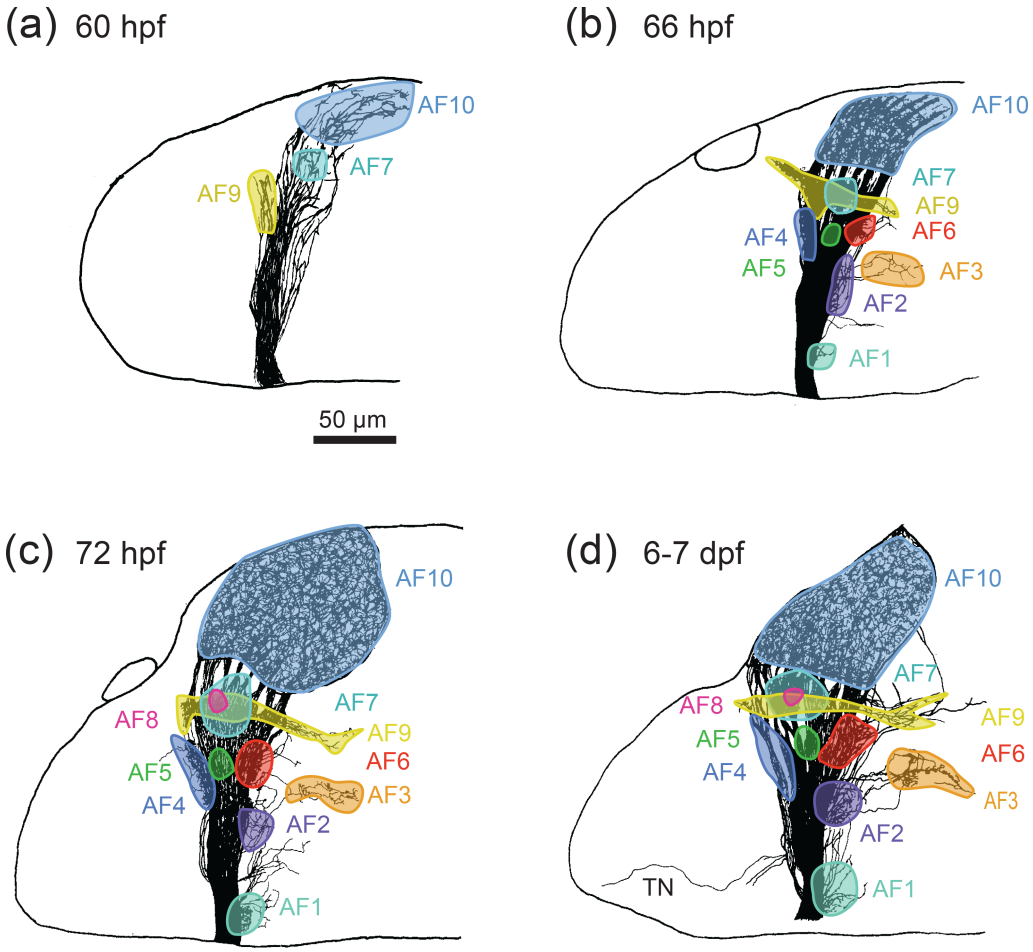

FIGURE 1 Burrill and Easter's (1994) original descriptions of retinofugal projections in zebrafish at embryonic and larval stages, based on wholemount specimens. The lipophilic tracer DiI was injected into the eye of a fixed embryo or larva and subsequently photoconverted to yield a brownish precipitate suitable for light microscopy. The developmental series shows that AFs form on the third day of development and then remain stable for days. (a) At 60 hpf, a first wave of RGC axons have reached the tectum (AF10). At the same time, precursors of AF7 and AF9 in the pretectum emerge. (b) At 66 hpf, all AFs have formed, with the possible exception of AF8. (c) By 72 hpf, the final AF pattern is visible. (d) The AF pattern remains stable up until the larval stage at which, currently, most behavioral and functional imaging experiments are carried out. AFs are color-coded similar to Figures 2 and 3. hpf, hours postfertilization; dpf, days postfertilization; TN, terminal nerve

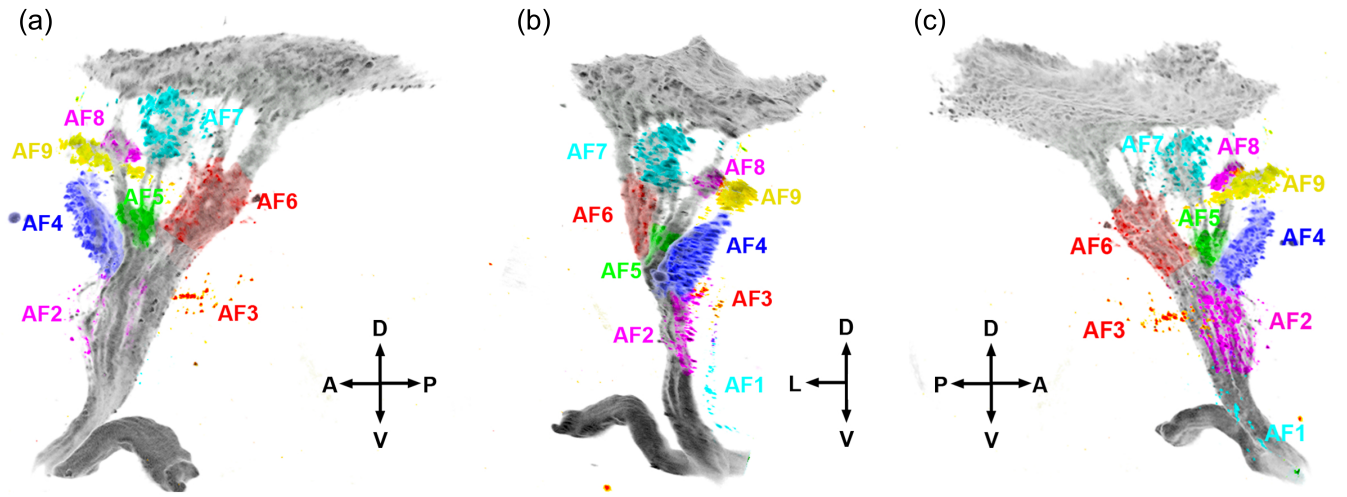

FIGURE 2 The retinal projectome of larval zebrafish. Robles et al. (2014) created a triple-transgenic zebrafish carrying *atoh7:Gal4-VP16* to drive expression of membrane-targeted mCherry (to label all RGC axons) and Synaptophysin-GFP (to label presynaptic terminals). Three views of the confocal image stack, taken at 6 dpf, are shown in (a)–(c). AFs are from the left side of the brain and are color-coded similar to Figures 1 and 3. A, anterior; P, posterior; D, dorsal; V, ventral; L, lateral

zebrafish RGCs using single-cell RNA sequencing and identified at least 33 molecularly distinct types with projection patterns that matched Robles et al.'s (2014) classification.

The AFs served as anatomical landmarks already in the first digital atlas of the larval zebrafish brain (z-brain; Randlett et al., 2015). Since then, a new digital atlas resource, mapzebrain (see Box 1), with added functionalities, has been developed, which combines transgene expression patterns and single-neuron tracings. This atlas shows the coordinates of AFs in a standardized, 3D reference space (Figure 3). In this review, we used the covisualization features of the atlas (see Box 1) to investigate the regional identity, cellular composition, and connectivity of each AF. Figure 4 illustrates how information from this digital resource can be tied to classical neuroanatomy. Three consecutive transverse sections from the mapzebrain atlas are shown in which the position of the AFs is indicated against a background of markers commonly used for neuroanatomical orientation: Synaptophysin as a neuropil stain and HuC (Elavl3) as a cell body stain for differentiated neurons (Figure 4a–c). Furthermore, the right panels show colocalization of AFs with three informative markers, which serve to compartmentalize the larval diencephalon: neurogenin (*ngn*), a marker of glutamatergic progenitors, tyrosine hydroxylase (*th*), a marker for catecholaminergic (here: dopaminergic) neurons, and glutamic acid decarboxylase isoform 1b (*gad1b/gad67*), a marker of GABAergic neurons (Figure 4a'–c'). These three sections encompass all 10 AFs and will be discussed further in Section 3.

The RNs or regions in the adult diencephalon and mesencephalon are well known in teleosts, including in cyprinids closely related to zebrafish, such as goldfish and carp (reviewed in Vanegas & Ito, 1983; Northcutt & Wullimann, 1988; Medina et al., 1993; Rupp et al., 1996; Wullimann, 1998). The positions and identities of RNs in adult zebrafish are depicted in Figure 5 (panels modified from Wullimann et al., 1996). The nomenclature follows Northcutt and Wullimann (1988), as discussed below. We have anglicized most of the anatomical descriptors; Latin adjectives or genitive forms (*preopticus*, *dorsalis*, *accessorius*, *thalami*, etc.) become English adjectives (preoptic, dorsal, accessory, thalamic, etc.). The RNs of adult zebrafish are listed in Table 1, together with their synonyms.

Burrill and Easter (1994) already attempted to draw correspondences between AFs and adult structures. However, these correlations turned out to be difficult to establish because, at early developmental periods, retinal terminal fields are within the neuropil located peripherally to the (largely not yet migrated) periventricular cell masses (see green neuropil areas in Figure 4). Thus, early AFs are not as closely associated anatomically with distinct visual diencephalic nuclei (i.e., neuronal cell body aggregates receiving retinal input; see red lettered structures in Figure 5) as is the situation in the adult brain. Thus, while it is almost trivial even in the larval zebrafish brain to identify the optic tectum (TeO) or the suprachiasmatic nucleus (SC) as recipients of terminal arborization fields AF10 or AF1, respectively, great uncertainties existed in establishing definitive one-to-one relationships between the remaining AFs 2 through 9 with any particular known adult RN. Since 1994, great advances have been made, both with respect to function, location, and connectivity of retinorecipient brain structures in larval zebrafish. We summarize the current status in this review.

In the next section (Section 2), we will first describe adult RNs in teleosts—in particular in cyprinids (including the zebrafish)—known from tract-tracing studies and also briefly summarize some relevant classical electrophysiological evidence. In Section 3, we will then proceed to the recent implementation of larval zebrafish AFs into the mapzebrain atlas using molecular markers contained in this atlas (Kunst et al., 2019) and give a first overall interpretation of the relationships of AFs to RNs. Section 4 relates modern neurobiological data on zebrafish visual subsystems to data from classical studies.

BOX 1 *mapzebrain*—Max Planck Zebrafish Brain Atlas

This atlas resource combines diverse, spatially resolvable data from the 6 dpf larval zebrafish brain and offers a range of online visualization and analysis tools. In its current version, the web portal at https://fishatlas.neuro.mpg.de exhibits three data modalities. The Regions subportal (a) shows 3D views of 112 anatomical regions, which segment the larval brain in a mutually exclusive, (nearly) collectively exhaustive fashion. Some of the masks are tentative in their current form, and the segmentation is continually improving as new data are considered. The Neurons subportal (b) allows the user to inspect over 4000 stochastically labeled neuronal morphologies, all collected from different, age-matched specimens and coregistered in a standard brain. Laterality of the cells (position in left or right brain hemisphere) is preserved in the atlas. The Markers subportal (c) lets the user interrogate over 400 transgenic reporter lines and a rapidly growing number (>100) of gene expression and antibody staining patterns. Regions, cells, and markers can be covisualized in any combination. Renditions can be rotated, clipped, and magnified to give the most informative views and colored in any desired way. The mapzebrain resource further enables the user to visualize multiple, selected structures across all data modalities, to create publication-ready images or animations, and to download the data for further analysis.

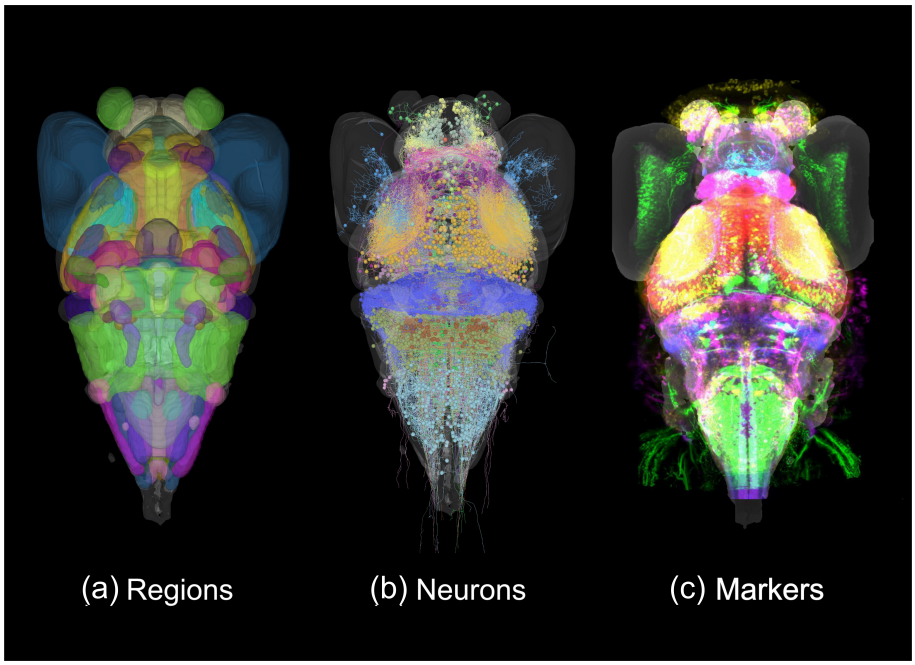

Finally, Section 5 presents mapzebrain atlas-based demonstrations of retinorecipient larval diencephalic (single-cell) neurons and their relation to particular AFs in newly visualized overall neuroanatomical context. Reassuringly, these single-cell reconstructions from the mapzebrain database corroborate the classical annotations and often extend the interpretation by predicting synaptic connectivity and function.

2 | RETINORECIPIENT NUCLEI IN THE ADULT TELEOST BRAIN

Although there is some variability in retinal targets among teleosts, the picture within cypriniforms is quite uniform with a series of adult RNs and targets common to all species studied (reviewed in Northcutt & Wullimann, 1988). We summarize briefly data on retinal projections in cyprinids gained with modern tract-tracing methods. Starting in the late 1970s, axonal tract-tracing methods included intraocular injections or optic nerve stump applications of [^{3}H] L-proline (with subsequent radioautography), *Phaseolus vulgaris*-leucoagglutinin (PHA-L), horseradish-peroxidase (HRP), biocytin, dextran amines and other substances in live brains as well as using lipophilic dyes (such as DiI, see above) in aldehyde-fixed brains (review on tract-tracing methods: Lanciego & Wouterlood, 2020).

In the 1970s, the standard neuroanatomical terminology used for cyprinids was that of Peter and Gill (1975) established in the goldfish (and beyond cyprinid species, for example, in the cyprinodont killifish; Peter et al., 1975). The goldfish was then the main neurobiological laboratory species for teleost brain research. However, Northcutt and Wullimann (1988) suggested a terminological revision of RNs based on Braford and Northcutt's (1983) new comparative concept of the cyprinid diencephalon. This diencephalic neuroanatomical terminology,

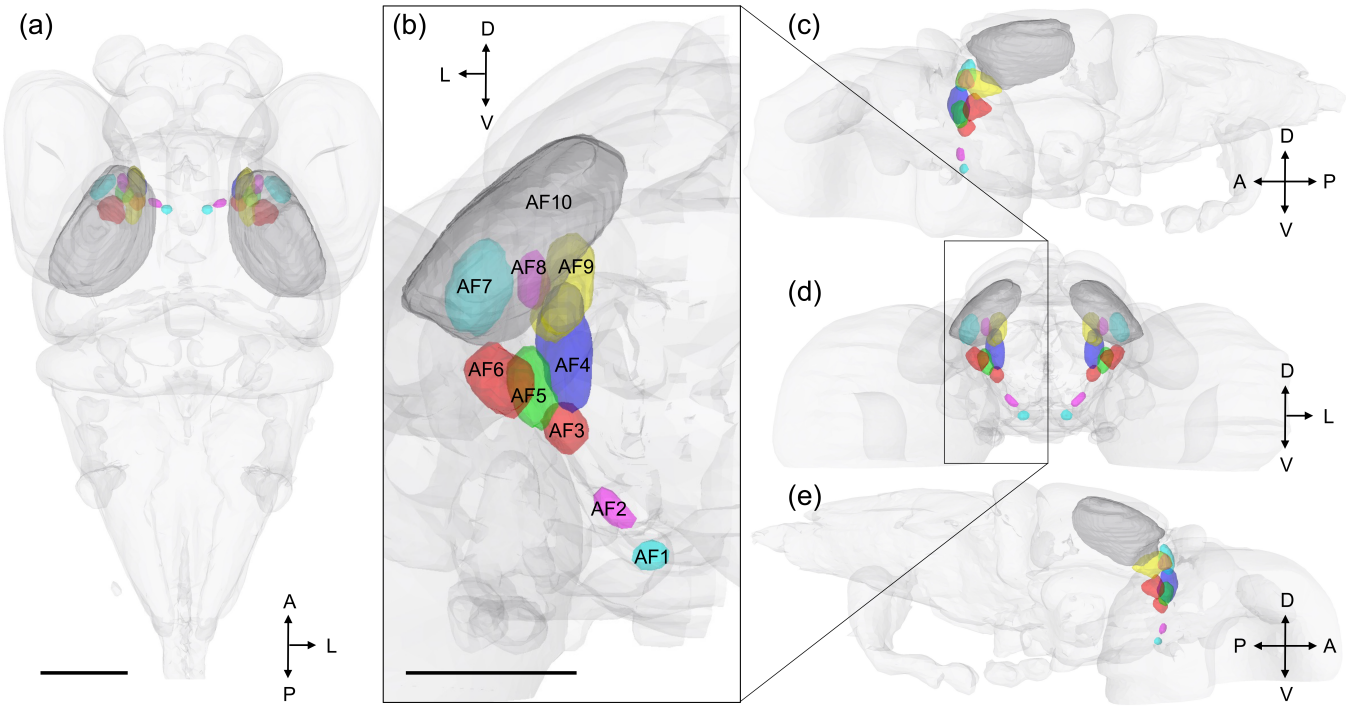

FIGURE 3 Retinorecipient AFs in the mapzebrain atlas. Snapshots of a 3D rotatable view generated by visualization tools at https://fishatlas.neuro.mpg.de. The atlas contains a fully segmented 6 dpf zebrafish brain in a standard reference space. The data modalities available in the atlas are annotated anatomical regions, including the 10 AFs (shown here), as well as ca. 4000 single neurons and 450 markers and transgenic lines, which can be covisualized in any desired combination. The atlas can be utilized for mapping functional imaging data or for classical neuroanatomy (see Figures 4, 6, 7 and 8). In (a), (c), (d) and (e), four different views of the AFs within a 3D rendition of the standard brain (light gray silhouette) are shown. (b) Higher magnification of the AF-containing subvolume of the standard brain is shown. AFs are color-coded similar to Figures 1 and 3. Scale bars in (a) and (b) are 100 μm. A, anterior; P, posterior; D, dorsal; V, ventral; L, lateral

together with Nieuwenhuys' (1963) classical telencephalic terminology, was later included and extended in the adult zebrafish brain atlas (Wullimann et al., 1996) and subsequently widely used in teleostean research papers, even in other brain atlasses, for example, for a swordtail fish (Anken & Rahmann, 1994), a pike (Means & Lannoo, 1996), the medaka (Anken & Bourrat, 1998), the sea bass (Cerdá-Reverter et al., 2001), the Japanese eel (Mukuda & Ando, 2003), a killifish (D'Angelo, 2013), and a cichlid (Simões et al., 2012).

Since the literature on teleostean retinal projections covers both the time period before and after this major terminological change, we shortly discuss the reasons for the change and introduce some main synonyms. Braford and Northcutt (1983) addressed critical misconceptions in the comparative understanding of the teleostean diencephalon by providing an improved neuroanatomy with a combined analysis of retinal projections in the goldfish. For example, two prominent nuclei in the dorsal thalamus of reptiles and birds, the nucleus geniculatus lateralis (NGL) and nucleus rotundus (NR), are relay nuclei of a retino-thalamo-pallial (NGL) and retino-tecto-thalamo-pallial (NR) pathway, respectively. These terms for sauropsid brains were used by Peter and Gill (1975) for the teleostean (retinorecipient) parvocellular and (tectorecipient) magnocellular superficial pretectal nuclei (PSp/PSm; see Figure 5). However, both teleostean nuclei have no ascending projections to the pallium as do the respective bird/reptilian thalamic NGL and NR (reviews: Braford & Northcutt, 1983; Northcutt & Wullimann, 1988; Wullimann, 1998). Furthermore, the teleostean PSp and PSm are most likely developmentally peripherally migrated from the periventricular pretectal histogenetic unit (see also Mueller & Wullimann, 2016) and not from the dorsal thalamic one. Thus, Braford and Northcutt (1983) proposed a general revision of the pretectum, which recognized a superficial (PSp/PSm, see above), a central pretectum (CPN; Peter and Gill's NC; probably meaning nucleus pretectalis centralis, abbreviation not explained) and a periventricular pretectum (PPd/v; see below). Both CPN and PPd/v are retinorecipient, as is the PSp (Braford & Northcutt, 1983). Furthermore, in the goldfish, a retinorecipient dorsal accessory optic nucleus (DAO; Northcutt & Wullimann, 1988; basal optic nucleus of Braford & Northcutt, 1983; nucleus pretectalis of Peter & Gill, 1975) and a ventral accessory optic nucleus (VAO; accessory optic nucleus of Braford & Northcutt, 1983; nucleus ventralis lateralis of Peter & Gill, 1975) were described. Of note, while the lateral geniculate nucleus is considered an anmniote novelty, the teleostean dorsal posterior thalamic nucleus may be homologous to the sauropsid nucleus rotundus (Striedter & Northcutt, 2020). All cyprinid RNs discussed are depicted for the adult zebrafish in Figure 5.

A related change applied to the teleostean thalamus (see Mueller, 2012), a region we refer to as "thalamus proper" in the mapzebrain atlas (https://fishatlas.neuro.mpg.de), to distinguish it from

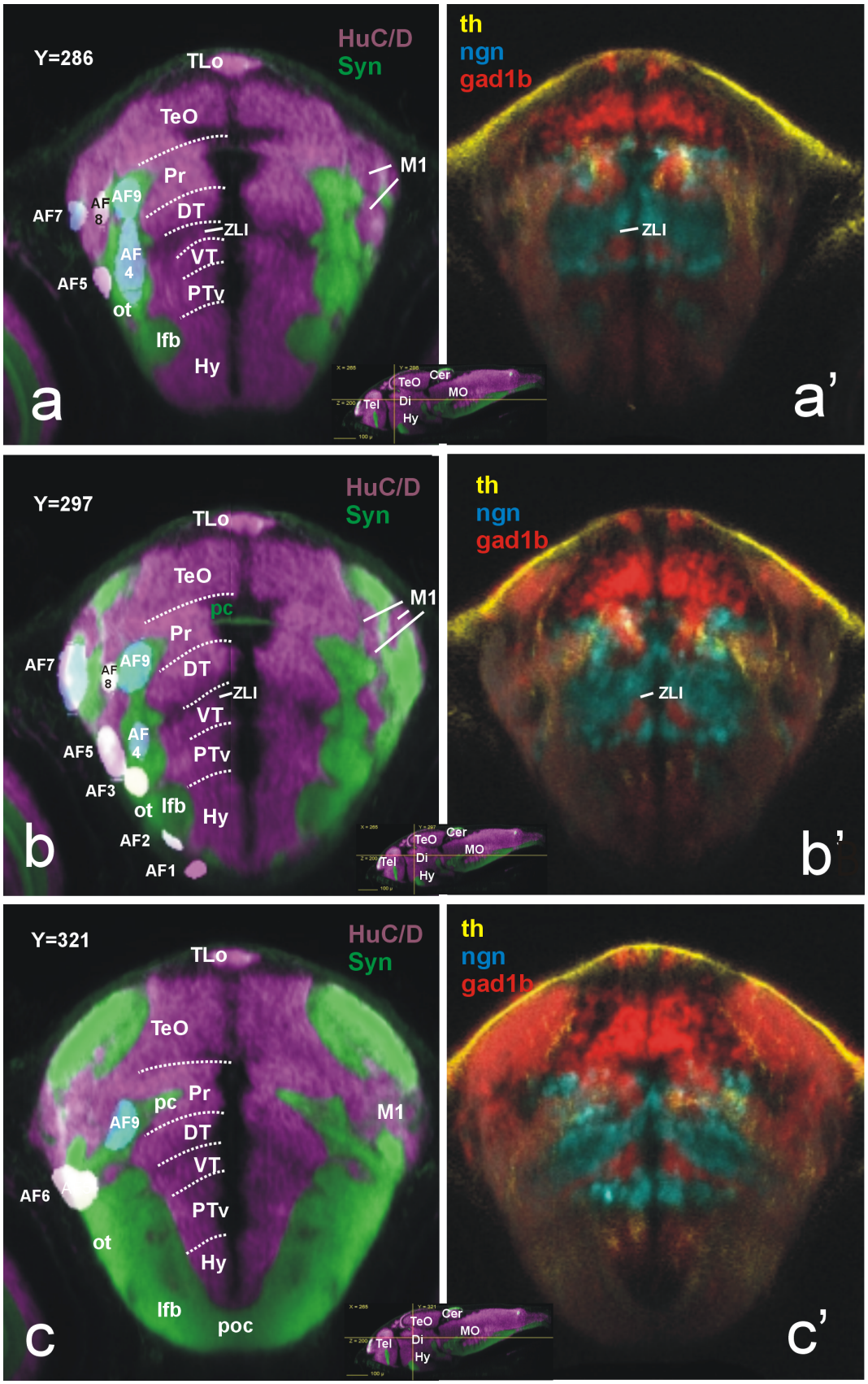

FIGURE 4 Legend on next page.

the basal and alar-most parts (habenula, epiphysis) of the dorsal thalamus prosomere. In order to improve the comparability within anamniotes, three main nuclei were described in the goldfish bearing great similarity to their counterparts in the amphibian thalamus: an anterior RN (A), and two (nonretinorecipient) more posterior nuclei, the dorsal posterior (DP) and central posterior (CP) thalamic nuclei (Braford & Northcutt, 1983; see Figure 5). Similarly, the (retinorecipient) ventral thalamus was revised to contain the intermediate (I), ventrolateral (VL), and ventromedial (VM) thalamic nuclei. In Peter and Gill's (1975) goldfish brain atlas, the three dorsal thalamic nuclei are contained in nucleus dorsolateralis and dorsomedialis thalami (NDL, NDM). Somewhat confusingly, Peter and Gill's (1975) NDL/NDM also include the most anterior part of the ventral thalamus (while the posterior part of the ventral thalamus is their nucleus ventromedialis, NVM) and, furthermore, the periventricular pretectal nucleus of the revised terminology (PPd/PPv; Figure 5d). Additionally, an area pretectalis is recognized in Peter and Gill's atlas (1975) in the relatively cell-sparse zone between VL and CPN which is not assigned to a nucleus in the revised terminology (see Figure 5). In the goldfish hypothalamic preoptic region, the commonly termed (retinorecipient) nucleus suprachiasmaticus (nucleus anterioris periventricularis-NAPv of Peter & Gill, 1975) and three additional preoptic subnuclei were recognized by Braford and Northcutt (1983), including the retinorecipient posterior parvocellular preoptic nucleus (PPp; Figure 5) (nucleus preopticus of Peter & Gill, 1975).

We will now describe zebrafish adult retinofugal nuclei, using this new terminology, and then shortly discuss further adult cyprinid retinofugal studies giving some additional important synonyms. Retinal projections in the adult zebrafish (Yáñez et al., 2009, 2018) conform to the general picture in cyprinids. For illustration, here we use the relevant levels of RNs (marked in red) as shown in the adult zebrafish brain atlas (Figure 5). Yáñez et al. (2009) report retinal fibers—after crossing brain sides in the optic chiasma—to ascend into the diencephalon where they form terminals lateral to the suprachiasmatic nucleus and the posterior parvocellular preoptic nucleus (SC/PPp; Figure 5a) before continuing toward ventral thalamus, dorsal thalamus and pretectum. Medially, retinal fibers diverge toward the ventrolateral thalamic nucleus (VL) (likely also reaching the intermediate thalamic nucleus, I) and anterior thalamic nucleus (located in the dorsal thalamus) (A; Figure 5a–c), as well as more caudally toward the dorsal periventricular pretectal nucleus (PPd; Figure 5d). The close-by (pretectal) paracommissural nucleus (PCN; Figure 5d) is also reported to receive retinofugal terminals (Yáñez et al., 2018). The remainder of retinal fibers continues to various layers of the optic tectum (TeO; not further discussed here, see Robles et al., 2013, and Robles et al., 2014). Retinofugal projections to the superficial pretectum (i.e., PSp), central pretectal nucleus (CPN) and the closely associated dorsal accessory optic nucleus (DAO) (Figure 5b,c) were later reported in the adult zebrafish by Yáñez et al. (2018). The neuropil directly rostrally adjacent to DAO receives input from the contralateral PSp (asterisk in Figure 5a; after Yáñez et al., 2018). The ventral accessory optic nucleus (VAO; Figure 5c) is located somewhat more caudally and was not reported as a retinal target in the adult zebrafish, but a retinorecipient VAO is reported in various other cyprinid species (see below).

Early, excellently detailed retinal projection studies in cyprinids (common roach *Rutilus rutilus* and carp, Repérant & Lemire, 1976; common rudd *Scardinius erythrophthalmus*, Repérant et al., 1976, Peyrichoux et al., 1977) reported in essence the same retinorecipient targets listed above for the zebrafish (the neuroanatomical terms for the rudd are given in parentheses below). Repérant and Lemire (1976) and Repérant et al. (1976) described as retinorecipient the PSp (then identified as nucleus geniculatus lateralis) and various additional pretectal nuclei corresponding to the PPd/PCN (centrum opticum commissurae posterioris), the CPN (centrum opticum pretectale dorsale), DAO (centrum opticum pretectale mediale + ventrale), VAO (centrum opticum accessorium), as well as the ventral and dorsal thalamus (centrum opticum dorsolaterale thalami) and the suprachiasmatic and posterior parvocellular preoptic nucleus (centrum opticum hypothalamicum). Interestingly, a VAO and an additional RN corticalis were only described in some predominantly visually guided cypriniforms in which the PSp was furthermore rather large (i.e., folded). These features are present in basal (e.g., salmon or pike) as well as derived (e.g., perches) teleosts (Butler et al., 1991) which supports the hypothesis that parts of the visual system are reduced in certain cypriniforms lacking them (e.g., zebrafish).

A few classical neurophysiological findings coming from single cell recordings related to retinorecipient teleost nuclei may be noted here. Dorsal and ventral thalamic neurons have large receptive fields, respond to stationary cues, are not directional, and do not habituate. Only ventral thalamic neurons may show bimodal (i.e., somatosensory-visual) responses (Friedlander, 1983). CPN neurons have small receptive fields, show no habituation, are directional in the horizontal plane, and respond best to slowly moving objects (Friedlander, 1983). Furthermore, pretectal neurons, clearly located in the goldfish CPN, are visually directional sensitive in both horizontal and vertical axes (Debowy & Baker, 2011; Masseck et al., 2010;

FIGURE 4 Three consecutive transverse levels from anterior to posterior, taken from the mapzebrain larval zebrafish brain atlas (https://fishatlas.neuro.mpg.de). Panels (a)–(c) depict AFs at their greatest extent with a HuC/D and Synapsin background, visualizing neuronal soma density and neuronal fibers, respectively. The registration process of HuC cells might underestimate the most peripheral cells and account for some peripherally located single cells shown in Figures 6–8 to be within the white matter. However, some single cells at the periphery of the gray matter might alternatively really be migrated into the white matter, as is typically the case in the preoptic region (see Figure 6a). Panels (a')–(c') show the same sections with molecular markers critical for compartmentalization of the diencephalon. See text for details. Cer, cerebellum; Di, diencephalon; DT, dorsal thalamus (thalamus); Hy, hypothalamus; lfb, lateral forebrain bundle; M1, early pretectal migration area; MO, medulla oblongata; ot, optic tract; poc, postoptic commissure; pc, posterior commissure; Pr, pretectum; PTv, posterior tuberculum, ventral part; Tel, telencephalon; TeO, optic tectum; TLo, torus longitudinalis; VT, ventral thalamus (prethalamus); ZLI, zona limitans intrathalamica

Masseck & Hoffmann, 2009a, 2009b) and implicated in the optokinetic reflex (see also Fite, 1985). Interestingly, a band of cells interconnects the CPN with the DAO (see Figure 5b,c) and retinal projections in the common roach cover both CPN and DAO, including this interconnecting band of cells, indicating that CPN and DAO may be functionally connected as an accessory optic system (AOS; see new data in zebrafish discussed in Section 3). This is supported by the fact that CPN/DAO and the interconnecting band of cells furthermore project to the corpus cerebelli in goldfish (Wullimann & Northcutt, 1988) and zebrafish (Yáñez et al., 2018; interpreted as intercalated pretectal nucleus Pi in their Figure 8d,e—a prerequisite for the optokinetic reflex—, while thalamic and hypothalamic nuclei do not have cerebellar projections. Interestingly, also VAO also projects to the cerebellum in goldfish and other teleosts (see Wullimann & Northcutt, 1988) indicating that it is a further functionally related nucleus. Based on connectivity and location, the DAO has been compared to the nucleus of the basal optic root in nonmammalian tetrapods and the mammalian medial terminal

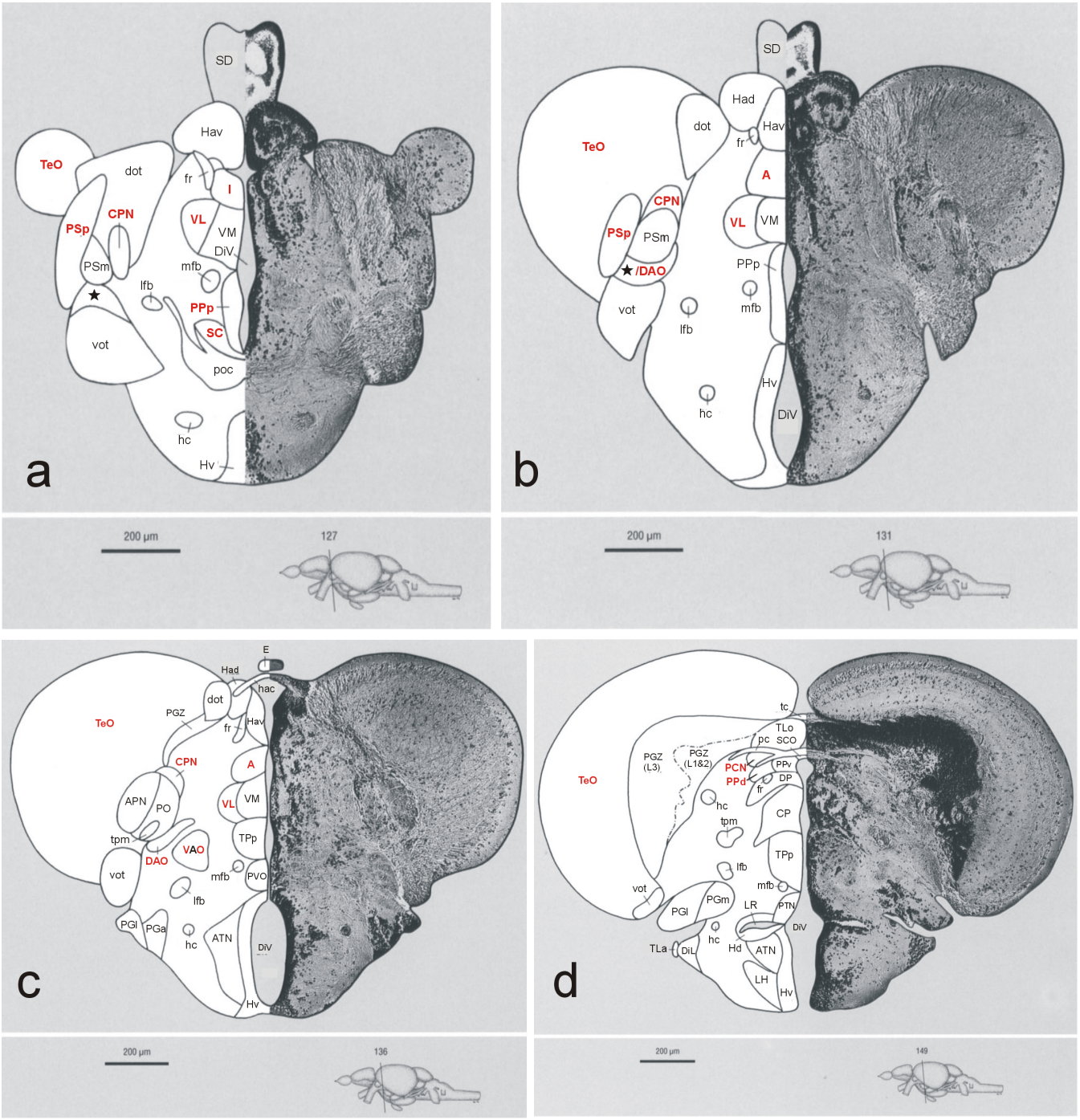

FIGURE 5 Legend on next page.

TABLE 1 Retinorecipient nuclei in the adult zebrafish and their likely associated arborization fields in the larva

Abbreviation	Adult nucleus/brain area (nomenclature used here)	Adult nucleus/brain area (old nomenclature)	Arborization field	Subdivision/ prosomere
SC	Suprachiasmatic nucleus	*Nucleus suprachiasmaticus*	AF1	Preoptic area
PPp	Posterior parvocellular preoptic nucleus	*Nucleus preopticus parvicellularis posterioris*	AF2	Preoptic area
VL	Ventrolateral thalamic nucleus	*Nucleus ventrolateralis thalami*	AF3/AF4	Ventral thalamus
I	Intermediate thalamic nucleus	*Nucleus intermedius thalami*	AF4	Ventral thalamus
A	Anterior thalamic nucleus	*nucleus anterioris thalami*	AF4	Dorsal thalamus
VAO	Ventral accessory optic nucleus	*Nucleus accessorius opticus ventralis*	AF6?	Pretectum?
DAO	Dorsal accessory optic nucleus	*Nucleus accessorius opticus dorsalis*	AF5	Pretectum
PSp	Parvocellular superficial pretectal nucleus	*Nucleus pretectalis superficialis pars parvicellularis*	AF7	Pretectum
CPN	Central pretectal nucleus	*Nucleus pretectalis centralis*	AF8	Pretectum
PCN	Paracommissural pretectal nucleus	–	AF9?	Pretectum
PPv	Ventral part of the periventricular pretectal nucleus	*Nucleus pretectalis periventricularis pars ventralis*	AF9v	Pretectum
PPd	Dorsal part of the periventricular pretectal nucleus	*Nucleus pretectalis periventricularis pars dorsalis*	AF9d	Pretectum
TeO	Optic tectum	*Tectum opticum*	AF10	Midbrain

nucleus, whereas the CPN resembles the avian nucleus lentiformis and the mammalian nucleus of the optic tract (discussed in Wullimann & Northcutt, 1988). However, the differential roles of adult CPN, DAO and VAO neurons in direction sensitivity and the optokinetic reflex may not be conserved and need further investigation.

3 | RETINORECIPIENT AFs IN THE MAPZEBRAIN ATLAS

The 10 larval AFs of Burrill and Easter (1994) were integrated into the mapzebrain atlas (Figure 3; https://fishatlas.neuro.mpg.de). AF4, AF5 and AF6 masks were imported from Kramer et al. (2019). Masks for AF1, AF2, AF3, AF8 and AF9 were drawn based on RGC axon labeling in an *isl2b:Gal4* x *UAS:mCherry* transgenic fish. The AF7 mask was segmented from a *vglut2a:DsRed* transgenic fish (M. Kunst, personal communication). Kernel density estimates of neuropil areas from six fish (Kramer et al., 2019) showed that size and absolute position of individual AFs vary by a few micrometers among individuals before averaging, while their relative positions along the optic tract are invariant.

Upon crossing brain sides, retinal fibers contribute massively to the large diencephalic neuropil located peripherally to the diencephalic cell masses (Figure 4; note that the optic chiasma is not shown, but lies between y-levels 297 and 321). This neuropil shows all fiber and neuropil masses (visualized in green with an anti-Synapsin marker). Thus, apart from retinal fibers, major additional fiber tracts are present in this neuropil, such as the medial and lateral forebrain

FIGURE 5 Consecutive transverse Cresyl-stained (cell somata) and Bodian Silver-impregnated (axonal fibers) sections, from anterior to posterior, of an adult zebrafish brain with all known retinofugal target nuclei (RNs) indicated in red. Modified after Wullimann, Rupp and Reichert: Neuroanatomy of the zebrafish brain. Birkhäuser, Basel (Wullimann et al., 1996). Asterisk denotes a neuropil receiving contralateral input from PSp (Yáñez et al., 2018). Note that VAO has not been confirmed as retinal target in adult zebrafish, but has in various other teleosts. See text for details. A, anterior thalamic nucleus; APN, accessory pretectal nucleus (of Wullimann & Meyer, 1990); ATN, anterior tuberal nucleus; CP, central posterior thalamic nucleus; CPN, central pretectal nucleus; DAO, dorsal accessory optic nucleus; DiL, diffuse nucleus of the inferior lobe; DiV, diencephalic ventricle; dot, dorsomedial optic tract; DP, dorsal posterior thalamic nucleus; E, epiphysis; fr, fasciculus retroflexus; hac, habenular commissure; Had, dorsal habenular nucleus; Hav, ventral habenular nucleus; hc, horizontal commissure; Hd, dorsal zone of periventricular hypothalamus; Hv, ventral zone of periventricular hypothalamus; I, intermediate thalamic nucleus; lfb, lateral forebrain bundle; LH, lateral hypothalamic nucleus; LR, lateral recess of diencephalic ventricle; mfb, medial forebrain bundle; pc, posterior commissure; PCN, paracommissural nucleus; PGa, anterior preglomerular nucleus; PGl, lateral preglomerular nucleus; PGm, medial preglomerular nucleus; PGZ, periventricular gray zone of optic tectum; PO, posterior pretectal nucleus (of Wullimann & Meyer, 1990); poc, postoptic commissure; PPd, dorsal periventricular pretectal nucleus; PPp, posterior parvocellular preoptic nucleus; PPv, ventral periventricular pretectal nucleus; PSm, magnocellular superficial pretectal nucleus; PSp, parvocellular superficial pretectal nucleus; PTN, posterior tuberal nucleus; PVO, paraventricular organ; SC, suprachiasmatic nucleus; SCO, subcommissural organ; SD, saccus dorsalis; tc, tectal commissure; TeO, tectum opticum; TeV, tectal ventricle; TLa, torus lateralis; TLo, torus longitudinalis; tpm, tractus pretectomamillaris; TPp, periventricular posterior tubercular nucleus; VAO, ventral accessory optic nucleus; VL, ventrolateral thalamic nucleus; VM, ventromedial thalamic nucleus; vot, ventrolateral optic tract

bundles that contain the telencephalic inputs and outputs. Most AFs lie as expected within this peripheral neuropil area. In contrast, the majority of larval neuronal cell bodies lies medial to these fiber/neuropil masses, with the exception of the peripherally migrated area M1 described previously as early pretectal migrated cell mass (M1; Mueller & Wullimann, 2005, 2016). M1 is the area of cell bodies wedged in between AF9 and AF7 and extending somewhat toward AF5 in Figure 4. Note that AF8 lies directly on neurons that form part of M1. However, the formation of distinct nuclei in the zebrafish larval brain is far from completed, which hampers the recognition of future adult RNs as described in Section 2.

We shall discuss now the extratectal retinal terminal fields (AFs 1 through 9) in the context of an improved understanding of developing histogenetic units in the larval zebrafish brain. The use of diagnostic markers such as *gad1b* (marker for GABAergic neurons), *ngn* (marker for glutamatergic neurons and their precursors), and *th* (marker for dopaminergic neurons) is critical for this analysis. The distribution of these and various additional markers has been studied by in situ hybridization and immunohistochemistry in detail in larval and adult zebrafish (Kaslin & Panula, 2001; Mueller et al., 2006, 2008; Mueller & Wullimann, 2003; Rink & Wullimann, 2001, 2002; Yamamoto et al., 2011, reviewed in Mueller & Wullimann, 2016). Together with morphological features (e.g., cell and neuronal somata density visualized by DAPI/Nissl stains or HuC, respectively) and landmarks such as ventricular shape or posterior and postoptic commissures, the molecular markers shown on the right-side panels (Figure 4) allow for compartmentalization of the diencephalon. While *gad1b* (red) expression is present massively in the optic tectum (TeO) and pretectum (Pr), it is largely absent from the dorsal thalamus (DT) where *neurogenin* (blue) is strongly expressed instead. Neurogenin-positive cells are also seen in the pretectum where tyrosine hydroxylase-positive cells (yellow) allow the pretectum to be differentiated from the dorsal thalamus. The ZLI is seen as a blackish stripe in Figure 4a,b and separates dorsal from ventral thalamus. The corresponding panels Figure 4a',b' on the right-side show that *gad1b* cells are again seen anterior to the ZLI. This *gad1b* domain represents the most posterior part of the ventral thalamus (VT). It is followed basally again by neurogenin-expressing cells within the posterior tuberculum (PT). The hypothalamus (Hy) shows yet only weak *gad1b* expression because of a prolonged proliferative activity at this stage (Mueller & Wullimann, 2002; Wullimann & Puelles, 1999).

In order to illustrate the AFs, we chose three coronal (transverse) levels which together depict all AFs at their greatest extent (Figure 4). The most anterior level A ($y = 286$) exhibits the AF4 at its greatest extent. Clearly, it lies lateral to both the periventricular cell masses of dorsal and ventral thalamus. AF7, AF8, and AF9 are also present at this level already and lie in the peripheral zone of the pretectal histogenetic unit. While AF9 is directly adjacent to the periventricular pretectal cells, AF7 and AF8 are associated with the early migrated pretectal area M1. AF5 lies lateral to AF4, but is also associated with adjacent migrated cell masses of pretectal origin (M1 of Mueller & Wullimann, 2005, 2016), as we shall confirm in Section 5.

Level B ($y = 297$) shows AFs 1 through 5 and 7 through 9. AF4 is at this level associated with the ventral thalamus only. This fits well with the fact that only the adult anterior (A), but not the posterior dorsal thalamic adult nuclei DP/CP; see Section 2) are retinorecipient. In contrast, the various pretectal AFs are most extensive at this level. While AF9 lies still immediately lateral to the periventricular pretectum, AF7 is most peripherally within the migrated pretectal M1 region and AF8 is directly on M1 cell bodies in-between AF9 and AF7. AF5 has its greatest extent at this level, still located basally to the M1 region and lateral to AF4. AF3 is basally adjacent. Also present at this level are AF1 which is directly adjacent to the suprachiasmatic part of the preoptic area and AF2 somewhat more dorsolateral in the preoptic region.

Level C ($y = 321$) finally shows AF6, but also still AF9. Thus, the latter has a very long anteroposterior extent, while the former only occurs at this caudal level essentially after AF5 has ended. Whereas AF9 is still directly lateral to the periventricular pretectum, AF6 lies again basal to the migrated M1 pretectal cell masses.

Generally, in vertebrates, incoming retinal fibers lie lateral to their retinorecipient diencephalic cell masses which extend dendrites into these terminal fields (Northcutt & Wullimann, 1988). In larval zebrafish, AF5, AF6, AF7 and, to a lesser degree, AF8 are located at the extreme lateral diencephalic periphery, at the edge of, or inside, M1, a pretectal migrated area. Thus, a first comparison of AFs and their association with the above-described anatomical diencephalic divisions using molecular markers and the adult neuroanatomy of RNs leads to the following interpretations:

- AF1 is the terminal field associated with the suprachiasmatic nucleus (adult SC).
- AF2 is the terminal field of the posterior parvocellular preoptic nucleus (adult PPp).
- AF3 appears like a basal extension of AF4 and is possibly associated with adult VL.
- AF4 is the terminal field likely associated both with dorsal thalamus (adult A) and ventral thalamus (adult VL).
- AF5/6 are in a position to qualify as likely terminal fields of adult DAO and VAO (see below).
- AF7 qualifies as terminal field of the adult PSp.
- AF8 is the terminal field directly on neurons qualifying as adult CPN.
- AF9 is the terminal field of the periventricular pretectum and likely also the paracommissural nucleus (adult PPd/PPv, PCN).
- AF10 is without doubt the neuropil of the optic tectum (TeO).

4 | FUNCTION OF THE RETINAL AFs

In the past decade, tremendous progress has been achieved in the functional neuroanatomy of the zebrafish larval visual system. Refined behavioral analysis, in combination with functional calcium imaging, lesion studies and optogenetic manipulations, have revealed the contribution of individual AFs to the processing of visual stimulus

TABLE 2 Responses to visual stimulus features of retinal axons terminating in AFs

Visual stimulus	AF4	AF5	AF6	AF7	AF8	AF9v	AF9d	AF10
Dimming/OFF	(10)		(1)		(1)	(2)		(3)
Brightening/ON	(4, 5)						(2)	(3)
Looming								(1, 3)
Moving grating		(6)	(7)					
Prey-like				(8)				(3, 8, 9)

Legend:
- Positive response shown.
- Response assumed, but anatomical annotation uncertain.
- No response detected.

Notes: References: (1) Temizer et al. (2015), (2) Robles et al. (2014), (3) Förster et al. (2020), (4) Zhang et al. (2017), (5) Lin and Jesuthasan (2017), (6) Kramer et al. (2019), (7) Naumann et al. (2016), (8) Semmelhack et al. (2014), (9) Bianco and Engert (2015), (10) Heap et al. (2018).

features and to behavioral responses (Table 2). In the following, we summarize the state of our knowledge, AFbyAF:

4.1 | AF1 and AF2

While the functions of SC (nucleus associated with AF1) and PPp (nucleus associated with AF2) have not been directly tested in zebrafish, they likely contribute to the photo-entrainment of circadian behavior, as they do in other vertebrates, including mammals (Güler et al., 2007; Rollag et al., 2003). One or both of these nuclei may also mediate visual background adaptation (VBA), a neuroendocrine response to ambient light, during which the skin lightens through a concentration of melanin granules in melanophores when animals are placed on a bright surface. VBA has been described in teleosts, amphibians and reptiles. In *Xenopus laevis*, light activates a subclass of intrinsically photosensitive retinal ganglion cells (ipRGCs), which express melanopsin (encoded by the *opn4* family of genes) and are enriched in the dorsal retina. These ipRGCs project to the preoptic area, from where the signal is further conveyed to melanotrope cells in the pituitary gland. This results in the inhibition of secretion of alpha-melanocyte stimulating hormone, a contraction of melanin granules in melanophores and an overall blanching of the animal (reviewed by Bertolesi and McFarlane, 2018).

While a homologous system has not yet been discovered in teleosts, VBA is disrupted in zebrafish that lack RGCs, for example, in *lakritz* mutants, in which complete loss of *atoh7* function prevents RGC neurogenesis (Kay et al., 2001), and in *blumenkohl* (*vglut2a*) mutants, in which synaptic transmission from RGCs is reduced (Smear et al., 2007). VBA is unaffected by mutations that eliminate photoreceptors or synaptic transmission in the outer retina (Muto et al., 2005; Neuhauss et al., 1999). Similar to *lakritz*, the *radar*^{s327} (*gdf6a*) mutant, in which dorsal RGCs do not develop, also shows pitch-black body coloration under all lighting conditions (Gosse and Baier, 2009), suggesting that the VBA is driven by RGCs in the dorsal retina, as it is in *X. laevis*.

A subpopulation of RGCs, which express the T-box transcription factor *eomesa* (*tbr2*), as well as *opn4a* and *opn4xa* (Kölsch et al., 2021), extend collaterals into AF1. Chemogenetic ablation of *eomesa*+ RGCs, using the nitroreductase/metronidazole system, did not produce a detectable deficit in VBA (Kölsch et al., 2021). Another subpopulation of *opn4*-expressing RGCs, which are negative for *eomesa* and positive for the transcription factor *onecut1*, are therefore, by exclusion, the best candidates for mediating VBA (K. Slanchev and H. Baier, unpublished observations). Taken together, we suspect that the VBA depends on inputs to either AF1 or AF2 from intrinsically photosensitive inner retinal cells, presumably ipRGCs in the dorsal retina, which express melanopsin (*opn4*) genes.

4.2 | AF3

Very little is known about the function of the associated nucleus, which is hypothesized here to be part of the ventral thalamus (see Section 5). A number of functional imaging experiments (Kramer et al., 2019; Kubo et al., 2014; Naumann et al., 2016; Wang et al., 2019; Wu et al., 2020) agree that AF3-projecting RGCs are not motion-sensitive or direction-selective.

4.3 | AF4

The most rostral retinorecipient neuropil is heavily innervated by RGCs (Robles et al., 2014). RGCs that arborize in AF4 continue to innervate

deep tectal layers, frequently forming collaterals in AF9 on their way to the tectum. A small subpopulation of RGCs (ca. 3% of all) terminates in AF4 and AF9 without further projections to the tectum. Imaging studies employing a battery of moving stimuli have not detected motion-sensitive, orientation-, or direction-selective responses. Zhang et al. (2017) reported that AF4 is contacted by ventral thalamic and/or thalamic eminence neurons, based on their observation that neurons extending dendrites into AF4 project to the left habenula (Turner et al., 2016). Thalamohabenular projections have been observed in goldfish and trout (Villani et al., 1996; Yañez & Anadón, 1996). Cells with dendrites in AF4 receive largely ON ganglion cell input, as shown by calcium imaging, project asymmetrically to the left habenula, and are required for light-seeking behavior (Zhang et al., 2017). Arriving at a similar conclusion, Cheng et al. (2017) and Lin and Jesuthasan (2017) demonstrated that blue, but not red, light activates a thalamic area, which projects to left habenula and includes AF4. Another candidate for these thalamic cells is the rostrolateral thalamic nucleus which is present in the adult zebrafish brain (Wullimann et al., 1996) and also projects to the habenula (Turner et al., 2016). However, this nucleus has neither been reported to receive retinal input in the adul zebrafish brain (see Section 2), nor do we see cells qualifying for it in our single cell larval brain analyses (see Section 5). In their behavioral assay, ablation of the area around AF4 abolished blue-light induced vertical migration up the water column. Recent molecular work corroborated AF4's contribution to light-seeking behavior or phototaxis. Chemogenetic ablation of an *eomesa*-expressing RGC subclass that projects to AF4 (among other AFs, including AF1 and AF9) and to the SAC/SPV layer of the optic tectum eliminated the zebrafish larva's phototaxis response to the lighter half of a dish (Kölsch et al., 2021).

The zebrafish visual thalamus has additional functions. Heap et al. (2018) demonstrated by functional imaging that a thalamic area responds to dimming of the visual scene, projects to the tectum, and determines the direction of escape from a looming threat. This nucleus might be the precursor of one of the adult RNs (A, I, or VL) in the larval thalamus. Moreover, some visual responses in the larval thalamus may have a tectal origin, although it is unclear if these would activate AF4 or an unknown tecto-thalamic neuropil. Our new anatomical analysis supports this more nuanced picture of AF4 (see Section 5). First, AF4 is probably a conglomerate neuropil harboring neurites of ventral thalamic and dorsal thalamic identities. All three thalamic RNs (A, VL, and I) probably contribute dendrites to AF4. Their respective neuropil compartments should separate later in development. If this scenario is correct, VL neuropil is split between AF3 and AF4 at larval stages.

4.4 | AF5

Calcium imaging showed that RGC terminals in AF5 respond strongly to visual motion in all directions (Kramer et al., 2019; Wang et al., 2019; Wu et al., 2020). Consonant with this observation, calcium imaging and tracing of single neurons demonstrated that direction-selective RGCs, which project to the superficial layers of the tectum (primarily SFGS1; Gabriel et al., 2012; Nikolaou et al., 2012), form collateral arbors in AF5 (Robles et al., 2014). The cell body-rich region dorsal to AF5/AF6 and ventral to AF9 responds strongly and selectively to binocular optic flow and is necessary and sufficient for optokinetic and optomotor responses (Kramer et al., 2019; Kubo et al., 2014). Therefore, deviating from Burrill and Easter (1994), who suggested that AF5 is the neuropil of a thalamic nucleus (without committing to any one in particular), we follow Kramer et al.'s (2019) interpretation that AF5 is probably the neuropil of DAO in the pretectum.

4.5 | AF6

AF6-projecting RGCs respond robustly to dark, looming stimuli, as well as to the gradual dimming of the entire visual field (Temizer et al., 2015), suggesting they are OFF-responsive. This is consistent with the stimulus preferences of tectal layers to which AF6-targeting RGC axons project, namely SFGS6 and SGC (Robles et al., 2014; Temizer et al., 2015). Other authors have recently argued that AF6 receives direction-selective inputs from the retina and is involved in the OMR (Naumann et al., 2016). This is inconsistent with the projection patterns of individual RGCs (Robles et al., 2014). RGCs that project to the direction-selective superficial layer SFGS1 of the tectum have not been observed to form collaterals in AF6, but rather in the adjacent AF5. Moreover, the zebrafish *radar*^{s327} (*gdf6a*) mutant (Gosse and Baier, 2009), in which dorsal RGCs do not develop and which lacks AF6, but retains AF5, is well able to perform responses to directional motion such as OKR and OMR (Muto et al., 2005). High-resolution calcium imaging showed that direction-selective inputs are found predominantly in AF5 (Kramer et al., 2019). A subset of pretectal cells that are responsive to optic flow extend axons into a dense neuropil area dorsal to, and partially overlapping with, AF6 (Kramer et al., 2019). Owing to the coarse imaging method and the unspecific transgenic line employed, Naumann et al. (2016) appear to have mis-annotated a large neuropil area, which includes this nonretinorecipient, but motion-responsive region, plus the neighboring AF5, as "AF6."

4.6 | AF7

Our anatomical considerations above arrived at the conclusion that AF7 is the neuropil of the larval PSp. Semmelhack et al. (2014) showed that AF7-projecting RGCs are tuned to characteristic features of prey stimuli, that is, the size and speed of small motile objects. Laser ablation of AF7 (Semmelhack et al., 2014) resulted in deficits in prey recognition, similar to lesion of the tectal neuropil (Gahtan et al., 2005). Laser dissection of the fascicle of RGC axons that collateralize in the tectal stratum opticum (SO) distal to AF7 also impaired responses to prey in the tectum (Förster et al., 2020). Strikingly, optogenetic activation of one, or very few, neurons that extend dendrites into AF7 was sufficient to elicit the initiation of hunting behavior (Antinucci et al., 2019). The transgenic line used for these experiments (*KalTAu508*) was investigated in the adult brain. Antinucci et al. (2019) found that at least some of the labeled neurons reside in the nonretinorecipient adult accessory pretectal nucleus (APN). Thus, if we assume continuity of the labeling pattern from larval to adult stages, larval APN cells may also contribute dendrites to AF7 neuropil. Laser ablation of

AF7 disrupted neither optomotor responses (Roeser & Baier, 2003; Semmelhack et al., 2014) nor phototaxis (Burgess et al., 2010).

In adult teleosts, no specific RN has been implicated in food perception or prey capture. Interestingly, a specific subpopulation of RGCs project to both AF7 and SO, the most superficial retinorecipient layer of the tectum (Robles et al., 2014). The same collateralization pattern was reported for RGCs in adult goldfish that project to the PSp (Springer & Mednick, 1985). In the retina, AF7-plus-SO-projecting RGCs exhibit either a narrow-diffuse or a bistratified dendrite morphology (Robles et al., 2014). Kölsch et al. (2021) showed that a subset of the RGC subclass that express the transcription factor *mafaa* exhibit these two morphologies. Some of them project to AF7 plus SO; another *mafaa*-positive subpopulation project to SFGS2. The tuning properties and function(s) of the five, or so, *mafaa*-expressing RGC types has so far not been investigated. We predict that a subset of them respond to prey features and are required for visual detection of prey.

Robles et al. (2014) demonstrated that AF7 receives inputs from RGCs located mainly in the temporal half of the retina. These projections are retinotopically organized. Thus, PSp/AF7 contains a map of the temporal visual field, which contains the area centralis, the zone that represents the prey image immediately before the capture strike (Mearns et al., 2020). RGCs in the area centralis are enriched for tuning to the ultraviolet (UV) range of the spectrum (Yoshimatsu et al., 2020). UV contrast likely aids in the detection of prey items (Flamarique & Hárosi, 2000). Interestingly, at least one *mafaa*-positive RGC subpopulation is enriched in the area centralis (Kölsch et al., 2021).

The neighboring PSm (see Figure 4b), which is not retinorecipient, projects to the hypothalamus. It is strongly innervated by an AF7-associated cell group and also receives projections from the optic tectum (in larval zebrafish: Muto et al., 2017; in adult carp: Yoshimoto & Ito, 1993). Thus, prey-responsive RGCs project to the AF7 neuropil region of PSp and, via collaterals, to the SO layer of the tectum; from both areas, information is passed on to PSm, which relays it to hypothalamic feeding centers.

4.7 | AF8

As described above, AF8 likely belongs to the central pretectal nucleus (CPN). Yáñez et al. (2018) confirmed in adult zebrafish that CPN is innervated by RGCs. In the larva, Temizer et al. (2015) showed that AF8-projecting RGCs respond to both dark looming disks and globally dimming stimuli, suggesting they respond to light offset. Consistent with their demonstrated physiology, Robles et al. (2014) described populations of mainly OFF-responsive RGC axons that formed collateral arbors in AF6 or AF8, before terminating in SFGS6 and SGC, two largely OFF-responsive layers of the tectum.

Very little is known about the function of CPN in adult fish. CPN neurons are activated by very slow horizontal motion (see Section 2). Masseck and Hoffmann (2009a) carried out electrophysiological recordings in goldfish pretectum and localized direction-selective responses to grating motion in a nucleus they called area praetectalis (APT). Judging by the drawings of the anatomical sections provided in this article, the APT corresponds to CPN. This raises the question if CPN (and by extension, AF8) is part of the optic-flow sensitive AOS. However, functional imaging studies in larval zebrafish have been unable to detect direction-selective or even motion-responsive RGC axons in AF8 (or neurons with this response profile near AF8). Such responses are abundant, however, in RGCs terminating in AF5, as well as in groups of pretectal cells around AF5/AF6. These neurons are substantially ventral to AF8. The latter position corresponds best to Masseck and Hoffmann's nucleus pretectalis (NP; Masseck & Hoffmann, 2009a) and is likely identical to our DAO. This apparent discrepancy can be resolved by the interpretation that Masseck and Hoffmann's APT is not directly innervated by RGCs; rather, the recorded cells may be postsynaptic to cells in DAO (which corresponds to their NP and, in zebrafish terminology, is associated with AF5). Alternatively, the tuning of AF8-projecting RGCs may be immature at the larval stages tested.

4.8 | AF9

Functional imaging studies have revealed that AF9, the neuropil of the periventricular pretectum, is further subdivided into an ON-responsive dorsal part, AF9d, and an OFF-responsive ventral part, AF9v (Robles et al., 2014). In some cypriniforms, including adult goldfish, a dorsal and a ventral nucleus can be anatomically distinguished. Both are innervated by RGC axons. We therefore propose that AF9d corresponds to PPd and AF9v to PPv. Yáñez et al. (2018) describe another retinorecipient pretectal nucleus, the paracommissural pretectal nucleus (PCN), in the periventricular pretectum (see Figure 5d). This nucleus was not considered by Burrill and Easter (1994). PCN either develops later or is at this stage fused with PPd and PPv. Kölsch et al. (2021) reported that *eomesa*-expressing RGCs, which constitute at least five different cell types, project to AF9. A similar diversity of morphologies and collateralization patterns was described for AF9-projecting RGCs by Robles et al. (2014). This is consistent with AF9 being a neuropil conglomerate of different pretectal nuclei.

Laser ablation of cells around AF9 was reported to reduce optomotor responses to grating motion (Semmelhack et al., 2014), and optogenetic activation of a similar region resulted in optokinetic-like eye movements (Kubo et al., 2014) and optomotor swimming in the absence of any visual stimulation (F. Kubo & H. Baier, unpublished observation). However, new results (Kramer et al., 2019; Wu et al., 2020) suggest that these earlier perturbations primarily affected cell populations that are immediately ventral to AF9 and may be associated with DAO/AF5.

4.9 | AF10

AF10 is the retinorecipient neuropil of the optic tectum (TeO). The tectum's broad function is well known; it is involved in sensorimotor tasks that require the localization and identification of visual objects, such as the approach of prey or the avoidance of obstacles. In zebrafish larvae, this was shown by functional imaging from RGC terminals and tectal

neurons (Bianco & Engert, 2015; Förster et al., 2020; Temizer et al., 2015) and in ablation studies by Roeser and Baier (2003), Gahtan et al. (2005) and Temizer et al. (2015). The tectum converts a retinotopic map of visual inputs into a map of directed motor outputs (shown in larval zebrafish by Helmbrecht et al., 2018).

Unilateral lesions of one tectum result in a curious reversal of light-seeking behavior, in that the fish with one tectum swim toward the dark (Burgess et al., 2010). This seemingly paradoxical result was elegantly explained by a contribution of OFF RGC inputs, which normally steer the fish in a direction away from the darker hemifield of the visual scenery (Burgess et al., 2010).

The tectum receives synaptic inputs from 97% of the RGCs (Robles et al., 2014), half of which are shared via collaterals with other AFs. Still, an intact AF10 is dispensable for responses to optic flow stimuli, such as optomotor or optokinetic reflexes, although it is involved in pacing of saccades during the OKR (Roeser & Baier, 2003). These behaviors, which compensate for self-motion, are probably driven by connections of direction-selective RGCs in the DAO of the pretectum without major contribution of the tectum.

5 | TRACING OF NEURONS THAT TARGET RETINAL AFs

This section explores the mapzebrain atlas for single cells (e.g., from Kunst et al., 2019, plus additional cells implemented by the Baier lab) and functionally defined neurons (e.g., direction-selective [DS] neurons of Kramer et al., 2019) regarding their neuroanatomical and connectional relationship to particular AFs. The basic search performed in the atlas is for neurons related to one of nine extratectal AFs (AF1 through AF9) in order to visualize cell somata with neurites (axons or dendrites) that terminate in a particular AF on both brain sides (respective AFs are shown in white in various figures). We assume as a working hypothesis that retrieved RGCs are always entering an AF with an axon and that single cells retrieved in ipsilateral diencephalic areas known as retinofugal targets (see Sections 2 and 3) enter the respective AFs with dendrites. Retrieved single cells that are more remote from an AF (e.g., tectal or rhombencephalic cells, but also contralateral diencephalic cells) more likely also extend axons rather than dendrites into an AF. Results are summarized in Table 3.

TABLE 3 Single cells extracted from mapzebrain atlas with a neurite into one particular AF

	AF2 (6)	AF3 (41)	AF4 (89)	AF5 (37)	AF6 (72)	AF7 (30)	AF8 (43)	AF9 (217)
Retina Re			4	7	3	2	3	7
Preoptic region P	**6**	1	2		1			1
Ventral thalamus		**25**		12	12			
Dorsal thalamus D			**58**			1	3	53
Hypothalamus H		1	1					3
Pretectum, periventricular Pr(p)		6	9			1		**129**
Pretectum, migrated Pr(M1)				**13**	**39**	**19**	**36**	
Optic tectum T		6	3	3	14	2	1	10
Midbrain tegmentum M			1					
Cerebellum C						1		1
Rhombencephalon R		2	10	2	4	2		13
Rhombencephalon-Nucleus isthmi R(I)						2		
Spinal ganglion S			1					

Notes: Top line shows AFs and total single cell number. Left column shows brain regions. Abbreviations after regions are used in figures to identify single cells, not the region itself. Highest single cell number for each AF in bold. Brackets show two areas for which not all cells were singly assigned, cell number is in predominant area of the two.

5.1 | AF1

The basic search for cell somata with a neurite into AF1 yields no results at the time this review was composed. Nonetheless, there is no doubt that this AF receives RGC input that is picked up by dendrites of suprachiasmatic (preoptic) neurons (see Sections 2 and 3). Likely, the absence of retrieved cells is a false negative result and can be explained by a regional bias in how single cells were entered into the atlas. This also explains that RGCs are only retrieved by basic searches in a fraction of other AFs (see below). Indeed, in their survey of almost 500 RGC projection patterns, Robles et al. (2014) described several RGCs with terminals in AF1, suggesting that RGCs are relatively undersampled in the mapzebrain atlas.

5.2 | AF2

The basic search for cell somata with a neurite into AF2 yields six neurons (Figure 6a), all of which are located in the preoptic region immediately anterior to AF2 (compare with Figure 4b). The transverse level (Figure 6a2) shows the exact histological position of one neuron on the left side (cyan) and one neuron on the right side (yellow). The remaining four bilaterally located neurons are slightly anterior to this transverse level as can be seen on the sagittal view (Figure 6a1). This sagittal level (Figure 6a1) is chosen as to show the main brain parts and anterior (ac) and postoptic (poc) commissures with the preoptic region in between and all cell somata were singly checked to confirm their exact histological position within the preoptic region using atlas coordinates in all three planes. Two neurons cross with a neurite (presumably an axon) to the other brain side. No retinal neurons are retrieved (see AF1 for explanation).

5.3 | AF3

The basic search for cell somata with a neurite into AF3 yields 41 neurons (Figure 6b), the majority of which (25) are located bilaterally in the ventral thalamus (VT). Six cells are in the periventricular pretectum

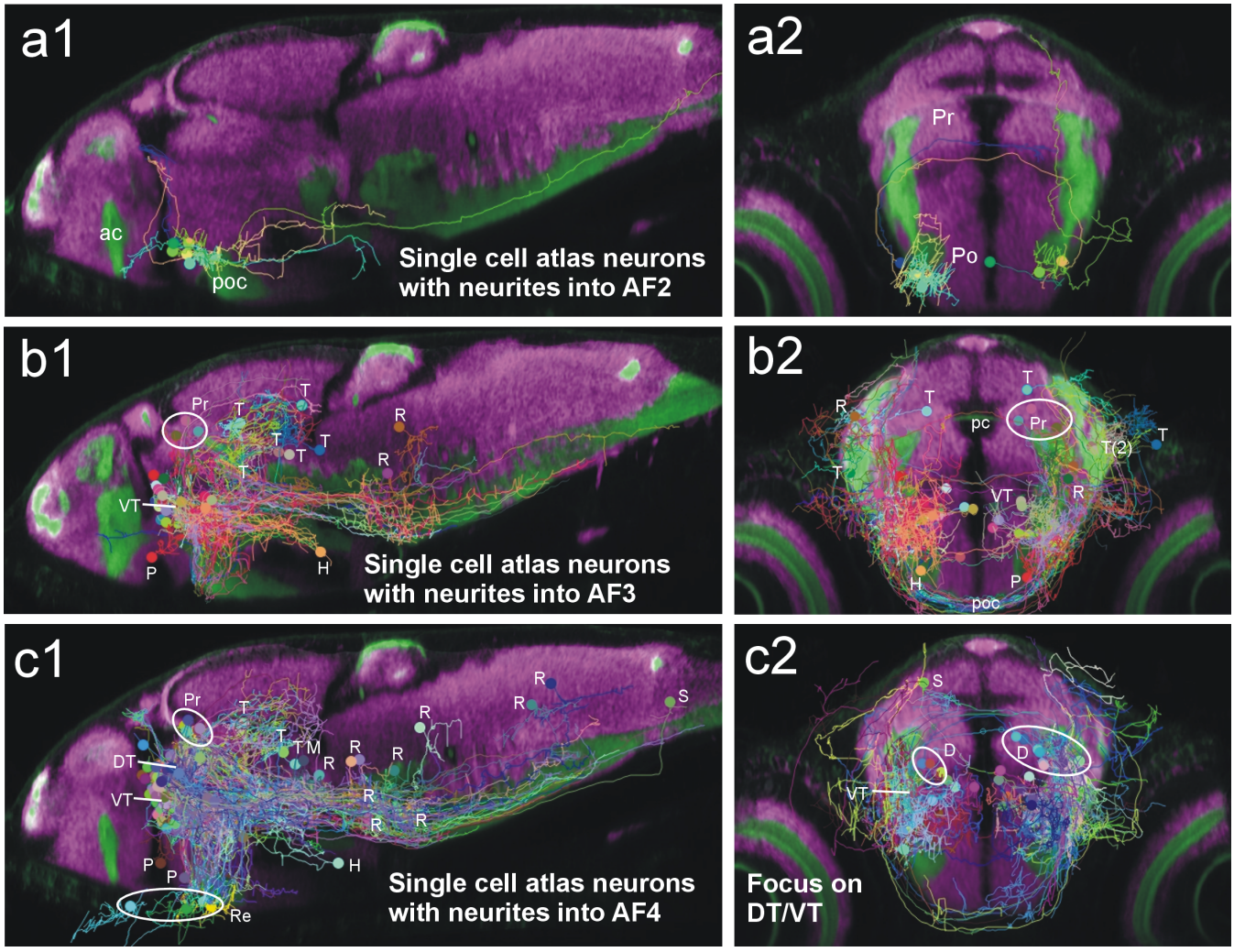

FIGURE 6 Single cells retrieved from mapzebrain atlas (e.g., of Kunst et al., 2019) that terminate with a neurite in AF2 (a), AF3 (b) or AF4 (c). White circles indicate more than one cell in a particular region. For details see text. ac, anterior commissure; D, dorsal thalamic cell; DT, dorsal thalamus; H, hypothalamic cell; M, midbrain tegmental cell; pc, posterior commissure; Po, preoptic region; poc, postoptic commissure; P, preoptic cell; Pr, pretectum; R, rhombencephalic cell; Re, retinal cell; S, spinal ganglion cell; T, tectal cell; VT, ventral thalamus

(Pr, three of four on the right brain side indicated by white circle), six cells in the optic tectum (singly indicated with T), two cells in the rhombencephalon (indicated with R), one cell in the inferior lobe of hypothalamus (indicated with H) and one cell in the preoptic region (indicated with P). This is already generally evident by comparing sagittal (Figure 6b1) and transverse (Figure 6b2) planes and is confirmed in detail by additional atlas searches for cells in each of those areas and by using atlas coordinates in three planes.

The transverse view (Figure 6b2) is the same level (y297) as also shown in Figure 4b in order to facilitate the general neuroanatomical localization of diencephalic neurons. The total of cells found to terminate with a neurite in AF3 are projected upon particular 2D planes shown for illustration. Thus, in order to reduce potential confusion particularly likely in the transverse plane (B2), tectal (T), rhombencephalic (R), hypothalamic (H), preoptic (P) and three right pretectal cells (Pr) are also indicated as in the sagittal view. Although the remaining cells are clearly concentrated in the ventral thalamus, the number and density of cell bodies require further checking for exact histological position. The atlas was then again used in all three planes using atlas coordinates to confirm the exact histological localization of dorsal and ventral thalamic cell body location. None of the 25 cells are in the dorsal thalamus, all neurons verified singly for exact histological position are in the ventral thalamus. Neurons that cross with a neurite to other brain side use the posterior, postoptic or ventral rhombencephalic commissures. No cells are retrieved in the retina (see AF1 for explanation).

5.4 | AF4

The basic search for cell somata with a neurite into AF4 yields 89 neurons, the overwhelming majority of which (58 cells) are located in the ventral and dorsal thalamus. Additional 31 cells are in other areas, that is, four cells in retina (Re, white circle in Figure 6c1), nine cells in the periventricular pretectum (four indicated with a white circle in C1), two cells in preoptic area (P), one cell in hypothalamus (H), three cells in optic tectum (all indicated with T), one cell in midbrain tegmentum (indicated with M), 10 cells in rhombencephalon (all indicated with R) and one cell apparently in an anterior spinal ganglion (S). The sagittal view (Figure 6c1) is slightly off the midline in order to show the main brain parts. Again, all cell bodies found are shown projected upon each of the 2D planes chosen. Thus, in order to facilitate recognition of thalamic cells, the other 31 cells (except for the spinal ganglion cell) were not shown in the transverse plane (Figure 6c2). The transverse view (Figure 6c2) is the same level (y286) as also shown in Figure 4a in order to allow for general neuroanatomical localization of thalamic neurons (if not specified further, the terms thalamic or thalamus are used for both dorsal and ventral thalamus in this Section). Additionally, atlas coordinates are used in all three planes to confirm the exact histological localization of many thalamic body locations. Seven (right side) and three (left side) dorsal thalamic cell somata are indicated with white circles in Figure 6c2. Most of the remaining cells in Figure 6c2 (except for S) are in the ventral thalamus. Retinal cells are bilaterally located (three on right side, one on left side) and their axons cross in the optic chiasm to the other brain side. Thalamic cell axons cross in the postoptic commissure, pretectal cells in posterior and postoptic commissures, tectal cell axons in the ansulate commissure, rhombencephalic cell axons cross in either postoptic or ventral rhombencephalic commissures, RGCs in the optic chiasma.

5.5 | AF5

The basic search for cell somata with a neurite into AF5 yields 37 single cells and the results are shown in Figure 7a in three planes. A general comparison of all three planes reveals that most of the retrieved cell somata are retinal and alar diencephalic cells. Among the latter are 13 pretectal cells (in the migrated pretectal area M1) and 12 thalamic cells which are all in the ventral thalamus (Figure 7a2). Seven cells are in the retina (white oval in Figure 7a1), two in rhombencephalon (all indicated with R in Figure 7a1) and three in optic tectum (all indicated with T in Figure 7a1). However, all cells found are shown projected upon one of each of these three 2D planes chosen. For example, the transverse view (Figure 7a2) shows the same level (y297) as also shown in Figure 4b in order to facilitate the general neuroanatomical localization of diencephalic neurons. Additionally, the atlas coordinates are then used in all three planes to confirm the exact histological localization of all retinal, tectal and rhombencephalic and many pretectal and ventral thalamic cell body locations. The sagittal view (Figure 7a1) is slightly off the midline in order to show the main brain parts. Retinal cells with a neurite (i.e., an RGC axon in this case) into AF5 lie only on the left side, unlike diencephalic single cells which are bilaterally located. Some of their neurites cross brain sides in the posterior (pc) or (mostly) postoptic commissures (poc). The horizontal plane (Figure 7a3) is chosen at the level of the posterior hindbrain neuron and, thus, shows its correct histological position. The exact position of the anterior rhombencephalic neuron and the three tectal neurons can be approximatively evaluated by comparing the three levels.

Next, we ask the atlas for all direction-selective (DS) neurons (studied and implemented into the atlas by Kramer et al., 2019). These are 58 cells located on the right side in dorsal thalamus and pretectum, mostly in the migrated pretectal area M1 (Figure 7b1), with very few cells also in the ventral thalamus, as can be verified by comparison of transverse (Figure 7b1) and sagittal (Figure 7b2) planes. Note that Figure 7b1 shows again the same transverse level y297 used also in Figure 4b, which facilitates the identification of neuroanatomical position of these DS neurons. These lie mostly posterior to this level, but the atlas coordinates are used to verify their position in pretectum, dorsal and ventral thalamus. The fact that the DS neuronal cell bodies lie on one brain side only and have no long axons (e.g., into cerebellum) is due to technical reasons.

Finally, we ask the atlas for those direction-selective neurons (of Kramer et al., 2019) that terminate with a neurite in AF5 (Figure 7c). The AF5 is shown on both brain sides in white in Figure 7b1,c1. This search yields three neurons and demonstrates that such DS neurons are exclusively in the migrated pretectal area M1.

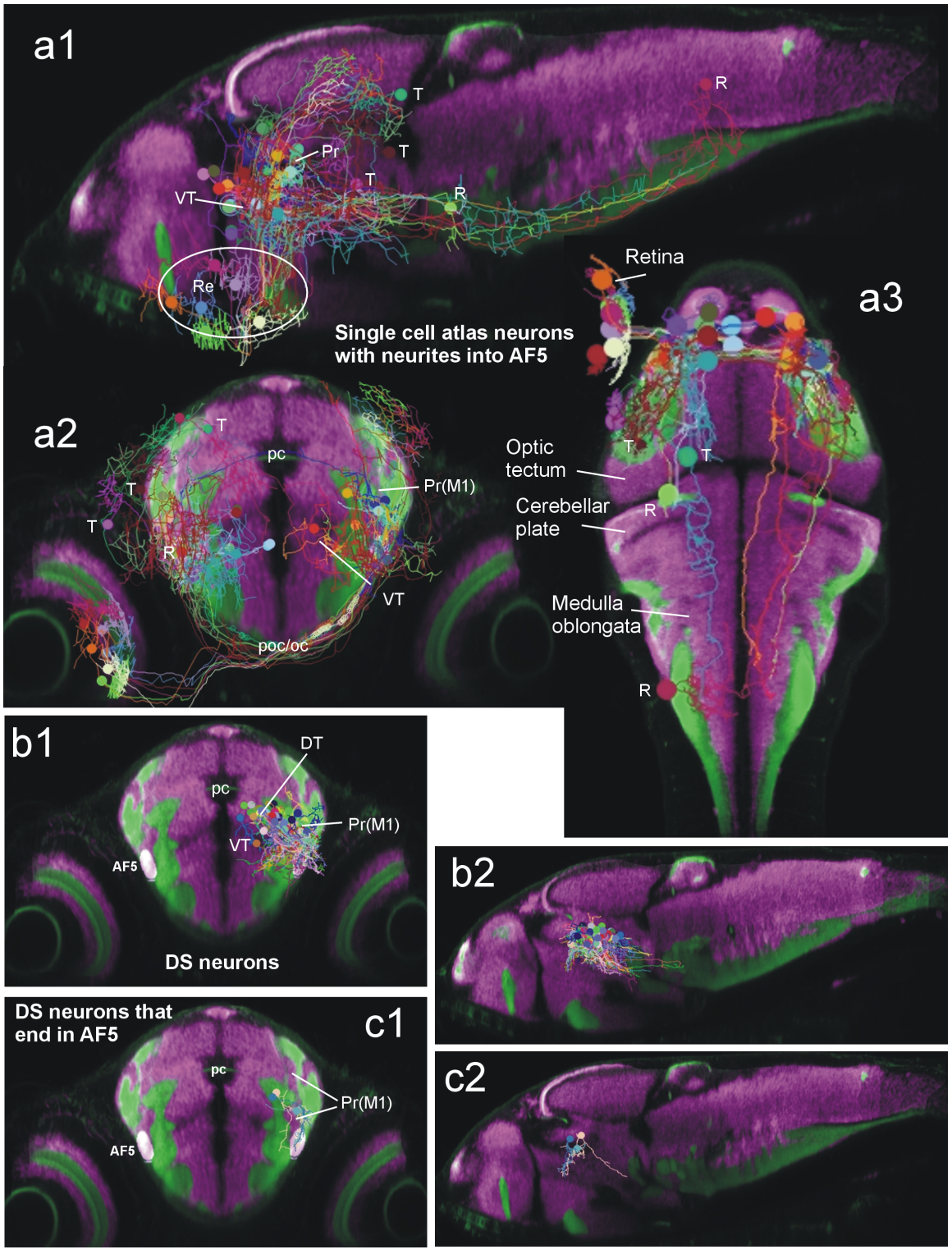

FIGURE 7 Single cells (e.g., of Kunst et al., 2019) that terminate with a neurite in AF5 (a) and related direction sensitive (DS) cells (of Kramer et al., 2019) that terminate in AF5 retrieved from mapzebrain atlas (b/c). White circle indicates retinal cells. For details see text. DT, dorsal thalamus; oc, optic chiasma; pc, posterior commissure; poc, postoptic commissure; Pr, pretectum; Pr(M1), cells in early migrated pretectal area; R, rhombencephalic cell; Re, retinal cell; T, tectal cell; VT, ventral thalamus

5.6 | AF6

The basic search for somata with a neurite into AF6 results in 72 neurons (Figure 8a1). Their distribution in the brain is qualitatively similar to those neurons found for AF5. The bulk of neurons is again in the alar diencephalon (39 mostly migrated pretectal M1 cells, see Figure 8a2, and 13 in thalamus, mostly in ventral thalamus, VT, one dorsal thalamic cell indicated with D in Figure 8a1) with a few

additional cells located in retina (Re, three cells), 14 in optic tectum (some indicated with T) and four in rhombencephalon (all indicated with R). Some pretectal cells project to the cerebellar corpus. Pretectal cells are mostly in the migrated pretectal area M1 with some in the periventricular pretectum Pr(p); Figure 8a2). Neurons which cross brain sides with an axon do so in the posterior, postoptic or ventral rhombencephalic commissure. The transverse level shown in Figure 8a2 is that of Figure 4c in order to facilitate neuroanatomical analysis. Atlas coordinates are used to confirm all retinal, tectal and rhombencephalic and many thalamic and pretectal cells.

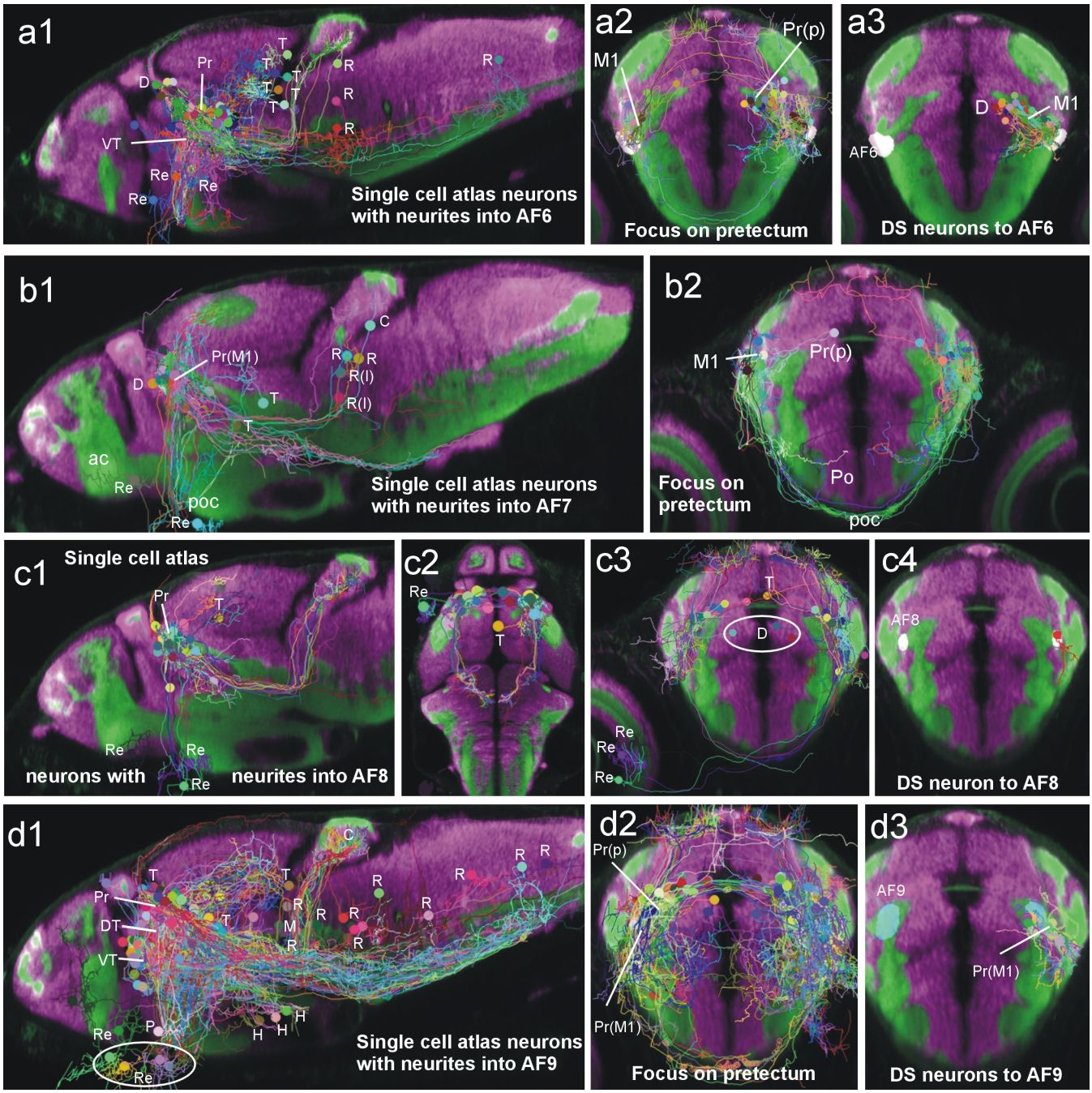

FIGURE 8 Single cells (e.g., Kunst et al., 2019) that terminate with a neurite in AF6 (a), AF7 (b), AF8 (c) and AF9 (d) and DS) neurons of Kramer et al. (2019) that terminate in some of these AFs retrieved from the mapzebrain atlas (b/c). White circles indicate more than one cell in a particular region. For details see text. ac, anterior commissure; C, cerebellar cell; D, dorsal thalamic cell; DT, dorsal thalamus; H, hypothalamic cell; M, midbrain tegmental cell; M1, cells in early migrated pretectal area pc posterior commissure; P, preaoptic cell; Po, preoptic region; poc, postoptic commissure; P, preoptic cell; Pr, pretectum; Pr(M1), cells in early migrated pretectal area; Pr(p), cells in periventricular pretectum; R, rhombencephalic cell; R(l), rhombencephalic cell in nucleus isthmi; Re, retinal cell; T, tectal cell; VT, ventral thalamus

A search for DS neurons (of Kramer et al., 2019) that terminate with a neurite into AF6 amounts to 18 cells, located predominantly in the pretectum (17 cells, mostly in the migrated pretectal area M1; Figure 8a3) with one cell in the dorsal thalamus (brown cell body, indicated with D).

5.7 | AF7

The basic search for somata with a neurite into AF7 yields 30 single cells (Figure 8b1), with a majority of 20 in pretectum (one cell in the periventricular pretectum (Pr-p) and the remaining cells in the migrated pretectal area M1; see Figure 8b2), one cell in dorsal thalamus (D, light brown cell body in Figure 8b1), two in retina (Re, one on each side), two in optic tectum (T, left side), one in cerebellum (C, left side), and four in rhombencephalon (R, two on both sides, including two nucleus isthmi—R(I)—cells). Again, the atlas coordinate system was used in three planes to verify exact histological position of all retinal, tectal and rhombencephalic and many thalamic and pretectal single cell bodies. Note that the left dark brown and right orange pretectal cell body shown in Figure 8b2 are both exactly in the transverse level (i.e., y297) within the migrated pretectal area M1. The sagittal view was again chosen off the midline to show main brain divisions. Some pretectal cells cross with an axon to the other brain side in the postoptic commissure. The RGCs use the optic chiasma to do so.

5.8 | AF8

The basic search for somata which terminate with a neurite in AF8 yields 43 neurons (Figure 8c1), with a majority of 36 pretectal cells (most of them in the migrated pretectal area M1 and one of which within AF8 itself, see also Figure 8c4), three retinal cells (Re), one tectal cell (T), and three dorsal thalamic cells (D, indicated with white circle in Figure 8c3). The RGCs are on the right side and the tectal cell on the left side, but alar diencephalic cells lie bilaterally. Again, level $y = 297$ is chosen for illustration and identification of neuroanatomical position, but all retinal, tectal dorsal thalamic, rhombencephalic and many pretectal cells were also singly verified for their position using atlas coordinates. Some pretectal cells cross with an axon to the other brain side in the posterior or postoptic commissures. The sagittal and horizontal views chosen furthermore show nicely that some pretectal cells project to the corpus cerebelli or optic tectum and some thalamic cells project to the optic tectum.

Finally, we visualize those DS neurons of Kramer et al. (2019) terminating with a neurite in AF8. One single neuron is found located directly adjacent to AF8 within the migrated pretectal area M1 (Figure 8c4).

5.9 | AF9

The basic search for cell somata with a neurite into AF9 yields 217 single cells total (Figure 8d1), with a majority of 129 pretectal cells (many in periventricular and migrated pretectal area M1, see Figure 8d2), seven retinal cells (three on left and four on right side), one preoptic cell, three hypothalamic cells, 10 cells in optic tectum and midbrain tegmentum, 13 in rhombencephalon and one in cerebellum (C). Neurons which cross brain sides with an axon do so in the posterior, postoptic, ansulate or ventral rhombencephalic commissures. Because of high cell density, only preoptic, other hypothalamic, cerebellar, tectal, midbrain tegmental, rhombencephalic, and retinal cells are verified individually using atlas coordinates in three planes. Some exemplary tectal (T) and rhombencephalic single cells are indicated in the sagittal view (Figure 8d1). Pretectal cells are shown separately in the transverse view (level: y297 again for neuroanatomical comparability with Figure 4b) many of which were also individually verified. This leaves 53 single cells in dorsal and ventral thalamus (summarily indicated in Figure 8d1) many of which were also verified individually. Furthermore, axonal projections to cerebellum and tectum originating in thalamus and pretectum are obvious.

When DS neurons of Kramer et al. (2019) with a neurite into AF9 are retrieved, these amount to 11, all located in the migrated pretectal area M1, none in the periventricular pretectum (Figure 8d3). Of note, additional searches for DS neurons of Kramer et al. (2019) with a neurite either into AF1, AF2, AF3, AF4, or AF7 yield no results.

5.10 | General observations on single-cell projection patterns

These single cell (basic) searches in the mapzebrain atlas were highly consistent with the analysis of larval and adult retinal targets and nuclei provided in Sections 2 through 4. The basic searches reveal in great detail where neurons with a neurite into particular AFs lie. As mentioned above, these neurites may theoretically be axons or dendrites, but we assume that neurons in larval diencephalic areas that are well known in adult teleosts, including the zebrafish, to be retinorecipient brain nuclei (described in Sections 2 and 3) have dendrites into an AF while others (such as RGCs, tectal, or rhombencephalic cells) project an axon into one or more AFs.

In all cases (i.e., AF2 through AF9; for AF1, see below), all (AF2) or the majority of single cells retrieved in each search are in that neuroanatomical diencephalic division as would be expected by the analysis presented in Sections 2 and 3. That is the preoptic region for AF2, the dorsal and ventral thalamus for AF4, the migrated pretectal area M1 for AF5, AF6, AF7, and AF8, and the periventricular pretectum for AF9. The cells retrieved for AF3 were predominantly in the ventral thalamus (see below for interpretation). These matches can be made because the majority of retrieved cells with dendrites into a particular AF always lie in one of these larval diencephalic areas. However, it seems that minor dendritic contacts to AFs from additional than the main diencephalic areas do occur. Whether these are real or false positive remains to be determined.

Long distance (i.e., axonal) inputs to AFs from retina, optic tectum and rhombencephalon are consistent with classical adult brain connectivity studies (see Section 3). One particularly nice example is the

input of nucleus isthmi cells to AF7 (Figure 8b1). Similarly, outputs of retrieved cells to cerebellum and medulla oblongata fit the adult connectivity picture, for example, only retrieved cells associated with AF6, AF8 and AF9 (i.e., adult DAO, CPN, PPd/PCN) project to the cerebellum (Figure 8a2,c1,d1), but not cells associated with AF2, AF3, AF4, or AF7 (i.e., adult PPp, VT, DT, PSp).

5.11 | Specific observations on single cells in preoptic region and dorsal/ventral thalamus

Although the search for AF1 targeting cells shows no results—certainly a result of the incomplete sampling of single cells in this region—, AF2 is clearly associated with preoptic cells located in a position of the adult posterior parvocellular preoptic nucleus (PPp). AF3 yields mostly cell bodies located in the ventral thalamus and none in the migrated pretectal region M1. This allows to conclude that AF3 is a ventral extension of AF4 and belongs to the retinothalamic neuropil and is thus not associated with the AOS. Moreover, AF4 is equally targeted by cells both in ventral and dorsal thalamus. Thus, AF4, and possibly also AF3, are input regions for both parts of the thalamus (adult anterior thalamic and ventrolateral/ventromedial thalamic nuclei, A, VL/VM in Figure 5).

5.12 | Specific observations on single cells in periventricular and superficial pretectum

Both basic searches for single cells contacting AF7 and AF9 retrieved a majority of cells in the pretectum, those for AF7 in the migrated pretectal area M1, those for AF9 mainly in the periventricular pretectum. This is consistent with their identification as adult parvocellular superficial pretectal nucleus (PSp) and dorsal periventricular pretectal nucleus (PPd) plus likely the paracommissural nucleus (PCN), respectively (see Figure 5).

5.13 | Specific observations on single cells in AOS

As suggested in Sections 2 and 3, the dorsal accessory optic nucleus (DAO) and central pretectal nucleus (CPN) form one retinorecipient structure only seemingly interrupted on some transverse levels by the magnocellular superficial pretectal nucleus (PSm, see Figure 5). Our basic searches demonstrate that neurons with neurites into AF5/AF6 and AF8 lie predominantly in the larval migrated pretectum M1 as expected for the future adult DAO and CPN. Moreover, a fraction of these are DS neurons that characterize functionally the AOS (Kramer et al., 2019). The one exemplary DS neuron targeting AF8 lies directly adjacent to the neuropil as expected for the adult central pretectal nucleus. The question whether there is a ventral accessory optic nucleus (VAO) in the zebrafish brain and how it is associated with an AF remains open at the moment. As discussed in Section 3, it has not been demonstrated in adult zebrafish and remains elusive in other (but not all) teleosts as well. It is furthermore highly interesting that no DS neurons are found associated with AF1 through AF4 (i.e., preoptic region and thalamus) and AF7 (superficial pretectum). This is expected from their known functional visual context different from direction selectivity (see Section 4).

6 | CONCLUSIONS

Much progress has been made in assigning functions to the retinofugal pathways in larval zebrafish. The retinal inputs to individual AFs have been traced, and their physiological responses to various features of visual stimuli have been recorded. As a result, most AFs can now be annotated with certainty in the framework of the well-established teleost neuroanatomy. Moreover, the knowledge of functional contributions of individual AF channels to visual processing is rapidly growing. Because AF4 and AF9 may each harbor two or three neuropil areas, respectively, it now emerges that 12–14 RNs are embedded in the original array of 10 AFs. This matches the number of RNs that was described in adult goldfish (Springer & Gaffney, 1981), a related cyprinid species, and in other teleosts (e.g., Northcutt & Wullimann, 1988). It is still unclear which diencephalic area is associated with AF6, although it appears likely that it is part of the larval AOS. Moreover, a paracommissural nucleus has not been identified in the larva. If it exists at 6 dpf its neuropil may be embedded in AF9. Future work is sure to shed light on these remaining questions. Much progress is expected to come from mapping molecularly defined RGC populations to individual AFs, from identifying diencephalic cell types and their connectivity, and from targeted genetic manipulations of inputs and outputs in the visual network of the larval zebrafish.

ACKNOWLEDGMENTS

We thank the members of our group for discussions and, in particular, Duncan Mearns, Johannes Larsch and Michael Kunst for comments. Estuardo Robles, Julia Kuhl, and Nawwar Mokayes assisted with preparation of Figures 1–3 and the figure in Box 1. Eva Laurell, Michael Kunst, Mariam Al Kassar and, particularly, Nawwar Mokayes generated and programmed the mapzebrain atlas. This work was funded by the Max Planck Society and the DFG (SFB 870, TP B16, reference number 118803580).

Open access funding enabled and organized by Projekt DEAL.

PEER REVIEW

The peer review history for this article is available at https://publons.com/publon/10.1002/cne.25204.

DATA AVAILABILITY STATEMENT

The data that support the findings of this study are openly available https://fishatlas.mpg.de

ORCID

Herwig Baier https://orcid.org/0000-0002-7268-0469
Mario F. Wullimann https://orcid.org/0000-0001-9292-2851

REFERENCES

Anken, R., & Bourrat, F. (1998). Brain atlas of the medakafish: *Oryzias latipes*. *INRA Editions* (pp. 91). 2-7380-0818-6.

Anken, R., & Rahmann, H. (1994). *Brain atlas of the adult swordtail fish Xiphophorus helleri and of certain developmental stages* (p. 88). Gustav Fischer.

Antinucci, P., Folgueira, M., & Bianco, I. H. (2019). Pretectal neurons control hunting behaviour. *eLife*, *8*, e48114. https://doi.org/10.7554/eLife.48114

Bertolesi, G. E., & McFarlane, S. (2018). Seeing the light to change colour: An evolutionary perspective on the role of melanopsin in neuroendocrine circuits regulating light-mediated skin pigmentation. *Pigment Cell Melanoma Res*, *31*(3), 354–373. https://doi.org/10.1111/pcmr.12678

Bianco, I. H., & Engert, F. (2015). Visuomotor transformations underlying hunting behavior in zebrafish. *Current Biology*, *25*(7), 831–846. https://doi.org/10.1016/j.cub.2015.01.042

Braford, M. R., & Northcutt, R. G. (1983). Organization of the diencephalon and pretectum of the ray-finned fishes. In R. E. Davis & R. G. Northcutt (Eds.), *Fish neurobiology: Higher brain areas and functions* (Vol. 2, pp. 117–163). University of Michigan Press.

Burgess, A. H., Schoch, H., & Granato, M. (2010). Distinct retinal pathways drive spatial orientation behaviors in zebrafish navigation. *Current Biology*, *20*(4), 381–386. https://doi.org/10.1016/j.cub.2010.01.022

Burrill, J. D., & Easter, S. S., Jr. (1994). Development of the retinofugal projections in the embryonic and larval zebrafish (*Brachydanio rerio*). *The Journal of Comparative Neurology*, *346*(4), 583–600. https://doi.org/10.1002/cne.903460410

Butler, A. B., Wullimann, M. F., & Northcutt, R. G. (1991). Comparative cytoarchitectonic analysis of some visual pretectal nuclei in teleosts. *Brain, Behavior and Evolution*, *38*(2–3), 92–114. https://doi.org/10.1159/000114381

Cerdá-Reverter, J. M., Zanuy, S., & Muñoz-Cueto, J. A. (2001). Cytoarchitectonic study of the brain of a perciform species, the sea bass (*Dicentrarchus labrax*). II. The diencephalon. *Journal of morphology*, *247*(3), 229–251. https://doi.org/10.1002/1097-4687(200103)247:3<229::AID-JMOR1014>3.0.CO;2-K

Cheng, R.-K., Krishnan, S., Lin, Q., Kibat, C., & Jesuthasan, S. (2017). Characterization of a thalamic nucleus mediating habenula responses to changes in ambient illumination. *BMC Biology*, *15*(1), 104. https://doi.org/10.1186/s12915-017-0431-1

D'Angelo, L. (2013). Brain atlas of an emerging teleostean model: *Nothobranchius furzeri*. *Anatomical Record (Hoboken, N.J. 2007)*, *296*(4), 681–691. https://doi.org/10.1002/ar.22668

Debowy, O., & Baker, R. (2011). Encoding of eye position in the goldfish horizontal oculomotor neural integrator. *Journal of Neurophysiology*, *105*(2), 896–909. https://doi.org/10.1152/jn.00313.2010

Fite, K. V. (1985). Pretectal and accessory-optic visual nuclei of fish, amphibia and reptiles: Theme and variations. *Brain, Behavior and Evolution*, *26*(2), 71–90. https://doi.org/10.1159/000118769

Flamarique, I. N., & Hárosi, F. I. (2000). Photoreceptors, visual pigments, and ellipsosomes in the killifish, *Fundulus heteroclitus*: A microspectrophotometric and histological study. *Visual Neuroscience*, *17*(3), 403–420.

Förster, D., Helmbrecht, T. O., Mearns, D. S., Jordan, L., Mokayes, N., & Baier, H. (2020). Retinotectal circuitry of larval zebrafish is adapted to detection and pursuit of prey. *eLife*, *9*, e58596. https://doi.org/10.7554/eLife.58596

Friedlander, M. J. (1983). The visual prosencephalon of teleosts. In R. E. Davis & R. G. Northcutt (Eds.), *Fish neurobiology. 2. Higher brain areas and functions* (pp. 91–115). University of Michigan Press.

Gabriel, J. P., Trivedi, C. A., Maurer, C. M., Ryu, S., & Bollmann, J. H. (2012). Layer-specific targeting of direction-selective neurons in the zebrafish optic tectum. *Neuron*, *76*(6), 1147–1160. https://doi.org/10.1016/j.neuron.2012.12.003

Gahtan, E., Tanger, P., & Baier, H. (2005). Visual prey capture in larval zebrafish is controlled by identified reticulospinal neurons downstream of the tectum. *The Journal of Neuroscience*, *25*(40), 9294–9303.

Gosse, N. J., & Baier, H. (2009). An essential role for Radar (Gdf6a) in inducing dorsal fate in the zebrafish retina. *Proc Natl Acad Sci USA*, *106*, 2236–2241. https://doi.org/10.1038/nature06816

Güler, A. D., Altimus, C. M., Ecker, J. L., & Hattar, S. (2007). Multiple photoreceptors contribute to nonimage-forming visual functions predominantly through melanopsin-containing retinal ganglion cells. *Cold Spring Harbor Symposia on Quantitative Biology*, *72*, 509–515. https://doi.org/10.1101/sqb.2007.72.074

Heap, L. A. L., Vanwalleghem, G., Thompson, A. W., Favre-Bulle, I., & Scott, E. K. (2018). Luminance changes drive directional startle through a thalamic pathway. *Neuron*, *99*(2), 293–301. https://doi.org/10.1016/j.neuron.2018.06.013

Helmbrecht, T. O., dal Maschio, M., Donovan, J. C., Koutsouli, S., & Baier, H. (2018). Topography of a visuomotor transformation. *Neuron*, *100*, 1429–1445.

Honig, M. G., & Hume, R. I. (1989). Carbocyanine dyes. Novel markers for labelling neurons. *Trends in Neurosciences*, *12*(9), 336–338.

Kaslin, J., & Panula, P. (2001). Comparative anatomy of the histaminergic and other aminergic systems in zebrafish (*Danio rerio*). *The Journal of Comparative Neurology*, *440*(4), 342–377. https://doi.org/10.1002/cne.1390

Kay, J. N., Finger-Baier, K. C., Roeser, T., Staub, W., & Baier, H. (2001). Retinal ganglion cell genesis requires lakritz, a zebrafish atonal homolog. *Neuron*, *30*, 725–736.

Kölsch, Y., Hahn, J., Sappington, A., Stemmer, M., Fernandes, A. M., Helmbrecht, T. O., Lele, S., Butrus, S., Laurell, E., Arnold-Ammer, I., Shekhar, K., Sanes, J. R., & Baier, H. (2021). Molecular classification of zebrafish retinal ganglion cells links genes to cell types to behavior. *Neuron*, *109*(4), 645–662.e9. https://doi.org/10.1016/j.neuron.2020.12.003

Kramer, A., Wu, Y., Baier, H., & Kubo, F. (2019). Neuronal architecture of a visual center that processes optic flow. *Neuron*, *103*, 1–15. https://doi.org/10.1016/j.neuron.2019.04.018

Kubo, F., Hablitzel, B., Dal Maschio, M., Driever, W., Baier, H., & Arrenberg, A. B. (2014). Functional architecture of an optic flow-responsive area that drives horizontal eye movements in zebrafish. *Neuron*, *81*, 1344–1359.

Kunst, M., Laurell, E., Mokayes, N., Kramer, A., Kubo, F., Fernandes, A. M., Förster, D., Dal Maschio, M., & Baier, H. (2019). A cellular-resolution atlas of the larval zebrafish brain. *Neuron*, *103*(1), 21–38.e5. https://doi.org/10.1016/j.neuron.2019.04.034

Lanciego, J. L., & Wouterlood, F. G. (2020). Neuroanatomical tract-tracing techniques that did go viral. *Brain Structure & Function*, *225*(4), 1193–1224. https://doi.org/10.1007/s00429-020-02041-6

Lin, Q., & Jesuthasan, S. (2017). Masking of a circadian behavior in larval zebrafish involves the thalamo-habenula pathway. *Scientific Reports*, *7*(1), 4104. https://doi.org/10.1038/s41598-017-04205-7

Masseck, O. A., Förster, S., & Hoffmann, K. P. (2010). Sensitivity of the goldfish motion detection system revealed by incoherent random dot stimuli: Comparison of behavioural and neuronal data. *PLoS One*, *5*(3), e9461. https://doi.org/10.1371/journal.pone.0009461

Masseck, O. A., & Hoffmann, K. P. (2009a). Question of reference frames: Visual direction-selective neurons in the accessory optic system of goldfish. *Journal of Neurophysiology*, *102*(5), 2781–2789. https://doi.org/10.1152/jn.00415.2009

Masseck, O. A., & Hoffmann, K. P. (2009b). Comparative neurobiology of the optokinetic reflex. *Annals of the New York Academy of Sciences*, *1164*, 430–439. https://doi.org/10.1111/j.1749-6632.2009.03854.x

Means, S. M., & Lannoo, M. J. (1996). Patterns and processes of brain diversification within esociform teleosts. *Journal of Morphology*, *229*(1), 23–57. https://doi.org/10.1002/(SICI)1097-4687(199607)229:1<23::AID-JMOR2>3.0.CO;2-Q

Mearns, D. S., Donovan, J. C., Fernandes, A. M., Semmelhack, J. L., & Baier, H. (2020). Deconstructing hunting behavior reveals a tightly coupled stimulus-response loop. *Current Biology*, *30*(1), 54–69.e9. https://doi.org/10.1016/j.cub.2019.11.022

Medina, M., Repérant, J., Ward, R., Rio, J. P., & Lemire, M. (1993). The primary visual system of flatfish: An evolutionary perspective. *Anatomy and Embryology*, *187*(2), 167–191. https://doi.org/10.1007/BF00171749

Mueller, T. (2012). What is the thalamus in zebrafish? *Frontiers in Neuroscience*, *6*, 64.

Mueller, T., Vernier, P., & Wullimann, M. F. (2006). A phylotypic stage in vertebrate brain development: GABA cell patterns in zebrafish compared with mouse. *The Journal of Comparative Neurology*, *494*(4), 620–634. https://doi.org/10.1002/cne.20824

Mueller, T., & Wullimann, M. F. (2002). BrdU-, neuroD (nrd)- and Hu-studies reveal unusual non-ventricular neurogenesis in the post-embryonic zebrafish forebrain. *Mechanisms of Development*, *117*(1–2), 123–135. https://doi.org/10.1016/s0925-4773(02)00194-6

Mueller, T., & Wullimann, M. F. (2003). Anatomy of neurogenesis in the early zebrafish brain. *Brain Research. Developmental Brain Research*, *140*(1), 137–155. https://doi.org/10.1016/s0165-3806(02)00583-7

Mueller, T., & Wullimann, M. F. (2005). *Atlas of early zebrafish brain development. A tool for molecular neurogenetics* (1st ed.). Elsevier.

Mueller, T., & Wullimann, M. F. (2016). *Atlas of early zebrafish brain development. A tool for molecular neurogenetics* (2nd ed.). Academic Press, Elsevier.

Mueller, T., Wullimann, M. F., & Guo, S. (2008). Early teleostean basal ganglia development visualized by zebrafish Dlx2a, Lhx6, Lhx7, Tbr2 (eomesa), and GAD67 gene expression. *The Journal of Comparative Neurology*, *507*(2), 1245–1257. https://doi.org/10.1002/cne.21604

Mukuda, T., & Ando, M. (2003). *Brain atlas of the Japanese eel: Comparison to other fishes* (Vol. 29, pp. 1–25). Mem Fac Integrated Arts and Sci, Hiroshima Univ, Ser. IV.

Muto, A., Lal, P., Ailani, D., Abe, G., Itoh, M., & Kawakami, K. (2017). Activation of the hypothalamic feeding centre upon visual prey detection. *Nature Communications*, *8*, 15029. https://doi.org/10.1038/ncomms15029

Muto, A., Orger, M. B., Wehman, A. M., Smear, M. C., Kay, J. N., Page-McCaw, P. S., Gahtan, E., Xiao, T., Nevin, L. M., Gosse, N. J., Staub, W., Finger-Baier, K., & Baier, H. (2005). Forward genetic analysis of visual behavior in zebrafish. *PLoS Genetics*, *1*, e66.

Naumann, E. A., Fitzgerald, J. E., Dunn, T. W., Rihel, J., Sompolinsky, H., & Engert, F. (2016). From whole-brain data to functional circuit models: The zebrafish optomotor response. *Cell*, *167*, 947–960.e20.

Neuhauss, S. C., Biehlmaier, O., Seeliger, M. W., Das, T., Kohler, K., Harris, W. A., & Baier, H. (1999). Genetic disorders of vision revealed by a behavioral screen of 400 essential loci in zebrafish. *The Journal of Neuroscience*, *19*(19), 8603–8615. https://doi.org/10.1523/JNEUROSCI.19-19-08603.1999

Nieuwenhuys, R. (1963). The comparative anatomy of the actinopterygian forebrain. *Journal für Hirnforschung*, *7*, 171–192.

Nikolaou, N., Lowe, A. S., Walker, A. S., Abbas, F., Hunter, P. R., Thompson, I. D., & Meyer, M. P. (2012). Parametric functional maps of visual inputs to the tectum. *Neuron*, *76*, 317–324.

Northcutt, R. G., & Wullimann, M. F. (1988). The visual system in teleost fishes. Morphological patterns and trends. In J. Atema, R. R. Fay, A. N. Popper, & W. N. Tavolga (Eds.), *Sensory biology of aquatic animals* (pp. 515–552). Springer.

Peter, R. E., & Gill, V. E. (1975). A stereotaxic atlas and technique for forebrain nuclei of the goldfish, *Carassius auratus*. *The Journal of Comparative Neurology*, *159*(1), 69–101. https://doi.org/10.1002/cne.901590106

Peter, R. E., Macey, M. J., & Gill, V. E. (1975). A stereotaxic atlas and technique for forebrain nuclei of the killfish, *Fundulus heteroclitus*. *The Journal of Comparative Neurology*, *159*(1), 103–127. https://doi.org/10.1002/cne.901590107

Peyrichoux, J., Weidner, C., Repérant, J., & Miceli, D. (1977). An experimental study of the visual system of cyprinid fish using the HRP method. *Brain Research 130*(3), 531–537. https://doi.org/10.1016/0006-8993(77)90114-7

Randlett, O., Wee, C. L., Naumann, E. A., Nnaemeka, O., Schoppik, D., Fitzgerald, J. E., Portuges, R., Lacoste, A. M. B., Riegler, C., Engert, F., & Schier, A. F. (2015). Whole-brain activity mapping onto a zebrafish brain atlas. *Nature Methods*, *12*(11), 1039–1046. https://doi.org/10.1038/nmeth.3581

Repérant, J., & Lemire, M. (1976). Retinal projections in cyprinid fishes: A degeneration and radioautographic study. *Brain, Behavior and Evolution*, *13*(1), 34–57. https://doi.org/10.1159/000123800

Repérant, J., Lemire, M., Miceli, D., & Peyrichoux, J. (1976). A radioautographic study of the visual system in fresh water teleosts following intraocular injection of tritiated fucose and proline. *Brain Research*, *118*(1), 123–131. https://doi.org/10.1016/0006-8993(76)90846-5

Rink, E., & Wullimann, M. F. (2001). The teleostean (zebrafish) dopaminergic system ascending to the subpallium (striatum) is located in the basal diencephalon (posterior tuberculum). *Brain Research*, *889*(1–2), 316–330. https://doi.org/10.1016/s0006-8993(00)03174-7

Rink, E., & Wullimann, M. F. (2002). Development of the catecholaminergic system in the early zebrafish brain: An immunohistochemical study. *Brain Research. Developmental Brain Research*, *137*(1), 89–100. https://doi.org/10.1016/s0165-3806(02)00354-1

Robles, E., Filosa, A., & Baier, H. (2013). Precise lamination of retinal axons generates multiple parallel input pathways in the tectum. *The Journal of Neuroscience*, *33*(11), 5027–5039. https://doi.org/10.1523/JNEUROSCI.4990-12.2013

Robles, E., Laurell, E., & Baier, H. (2014). The retinal projectome reveals brain-area-specific visual representations generated by ganglion cell diversity. *Current Biology*, *24*, 2085–2096.

Roeser, T., & Baier, H. (2003). Visuomotor behaviors in larval zebrafish after GFP-guided laser ablation of the optic tectum. *The Journal of Neuroscience*, *23*, 3726–3734.

Rollag, M. D., Berson, D. M., & Provencio, I. (2003). Melanopsin, ganglion-cell photoreceptors, and mammalian photoentrainment. *Journal of Biological Rhythms*, *18*(3), 227–234. https://doi.org/10.1177/0748730403018003005

Rupp, B., Wullimann, M. F., & Reichert, H. (1996). The zebrafish brain: A neuroanatomical comparison with the goldfish. *Anatomy and Embryology*, *194*, 187–203.

Semmelhack, J. L., Donovan, J. C., Thiele, T. R., Kuehn, E., Laurell, E., & Baier, H. (2014). A dedicated visual pathway for prey detection in larval zebrafish. *eLife*, 3.

Simões, J. M., Teles, M. C., Oliveira, R. F., Van der Linden, A., & Verhoye, M. (2012). A three-dimensional stereotaxic MRI brain atlas of the cichlid fish *Oreochromis mossambicus*. *PLoS One*, *7*(9), e44086. https://doi.org/10.1371/journal.pone.0044086

Smear, M. C., Tao, H. W., Staub, W., Orger, M. B., Gosse, N. J., Liu, Y., Takahashi, K. D., Poo, M. M., & Baier, H. (2007). Vesicular glutamate transport at a central synapse limits the acuity of visual perception in zebrafish. *Neuron*, *53*, 65–77.

Springer, A. D., & Gaffney, J. S. (1981). Retinal projections in the goldfish: A study using cobaltous-lysine. *The Journal of Comparative Neurology*, *203*, 401–424.

Springer, A. D., & Mednick, A. S. (1985). Topography of the retinal projection to the superficial pretectal parvicellular nucleus of goldfish: A cobaltous-lysine study. *The Journal of Comparative Neurology*, *237*, 239–250.

Striedter, G., & Northcutt, R. G. (2020). *Brains through time: A natural history of vertebrates* (p. 540). Oxford University Press.

Temizer, I., Donovan, J. C., Baier, H., & Semmelhack, J. L. (2015). A visual pathway for looming-evoked escape in larval zebrafish. *Current Biology*, *25*, 1823–1834.

Turner, K. J., Hawkins, T. A., Yáñez, J., Anadón, R., Wilson, S. W., & Folgueira, M. (2016). Afferent connectivity of the zebrafish habenulae. *Frontiers in Neural Circuits*, *10*, 30. https://doi.org/10.3389/fncir.2016.00030

Vanegas, H., & Ito, H. (1983). Morphological aspects of the teleostean visual system: A review. *Brain Research*, *287*(2), 117–137. https://doi.org/10.1016/0165-0173(83)90036-x

Villani, L., Zironi, I., & Guarnieri, T. (1996). Telencephalo-habenulo-interpeduncular connections in the goldfish: A DiI study. *Brain, Behavior and Evolution*, *48*, 205–212.

Wang, K., Hinz, J., Haikala, V., Reiff, D. F., & Arrenberg, A. B. (2019). Selective processing of all rotational and translational optic flow directions in the zebrafish pretectum and tectum. *BMC Biology*, *17*(1), 29. https://doi.org/10.1186/s12915-019-0648-2

Wu, Y., Dal Maschio, M., Kubo, F., & Baier, H. (2020). An optical illusion pinpoints an essential circuit node for global motion processing. *Neuron*, *108*, 1–13.

Wullimann, M. F. (1998). The central nervous system. In D. H. Evans (Ed.), *Physiology of fishes* (pp. 245–282). CRC Press.

Wullimann, M. F., & Meyer, D. L. (1990). Phylogeny of putative cholinergic visual pathways through the pretectum to the hypothalamus in teleost fish. *Brain, Behavior and Evolution*, *36*(1), 14–29. https://doi.org/10.1159/000115294

Wullimann, M. F., & Northcutt, R. G. (1988). Connections of the corpus cerebelli in the green sunfish and the common goldfish: A comparison of perciform and cypriniform teleosts. *Brain, Behavior and Evolution*, *32*(5), 293–316. https://doi.org/10.1159/000116558

Wullimann, M. F., & Puelles, L. (1999). Postembryonic neural proliferation in the zebrafish forebrain and its relationship to prosomeric domains. *Anatomy and Embryology*, *199*(4), 329–348. https://doi.org/10.1007/s004290050232

Wullimann, M. F., Rupp, B., & Reichert, H. (1996). *Neuroanatomy of the zebrafish brain. A topological atlas*. Birkhäuser.

Yamamoto, K., Ruuskanen, J. O., Wullimann, M. F., & Vernier, P. (2011). Differential expression of dopaminergic cell markers in the adult zebrafish forebrain. *The Journal of Comparative Neurology*, *519*(3), 576–598. https://doi.org/10.1002/cne.22535

Yañez, J., & Anadón, R. (1996). Afferent and efferent connections of the habenula in the rainbow trout (*Oncorhynchus mykiss*): An indocarbocyanine dye (DiI) study. *The Journal of Comparative Neurology*, *372*, 529–543.

Yáñez, J., Busch, J., Anadón, R., & Meissl, H. (2009). Pineal projections in the zebrafish (*Danio rerio*): Overlap with retinal and cerebellar projections. *Neuroscience*, *164*(4), 1712–1720. https://doi.org/10.1016/j.neuroscience.2009.09.043

Yáñez, J., Suárez, T., Quelle, A., Folgueira, M., & Anadón, R. (2018). Neural connections of the pretectum in zebrafish (*Danio rerio*). *The Journal of Comparative Neurology*, *526*, 1017–1040.

Yoshimatsu, T., Schröder, C., Nevala, N. E., Berens, P., & Baden, T. (2020). Fovea-like photoreceptor specializations underlie single UV cone driven prey-capture behavior. *Neuron*, *107*(2), 320–337.e6.

Yoshimoto, M., & Ito, H. (1993). Cytoarchitecture, fiber connections, and ultrastructure of the nucleus pretectalis superficialis pars magnocellularis (PSm) in carp. *The Journal of Comparative Neurology*, *336*(3), 433–446. https://doi.org/10.1002/cne.903360309

Zhang, B., Yao, Y., Zhang, H., Kawakami, K., & Du, J. (2017). Left habenula mediates light-preference behavior in zebrafish via an asymmetrical visual pathway. *Neuron*, *93*, 914–928.e4.

How to cite this article: Baier, H., & Wullimann, M. F. (2021). Anatomy and function of retinorecipient arborization fields in zebrafish. *Journal of Comparative Neurology*, *529*(15), 3454–3476. https://doi.org/10.1002/cne.25204